Evolving shipping activity in climate scenarios

Coupling econometrics with Integrated Assessment Model

Naghash, Hesam; Schott, Dingena; Pruyn, Jeroen

DOI
10.1016/j.oceaneng.2025.120516

Publication date
2025

Document Version
Final published version

Published in
Ocean Engineering

Ocean Engineering 322 (2025) 120516

Contents lists available at ScienceDirect

Ocean Engineering

journal homepage: www.elsevier.com/locate/oceaneng

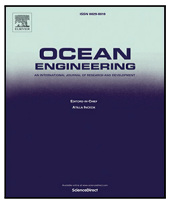

Research paper

Evolving shipping activity in climate scenarios: Coupling econometrics with Integrated Assessment Model☆

Hesam Naghash *, Dingena Schott [1], Jeroen Pruyn [1]

Maritime and Transport Technology, TU Delft, Mekelweg 2, 2628CD, Delft, Netherlands

ARTICLE INFO

Keywords:
International shipping
Shipping demand
Climate change
Integrated assessment modeling
CO_2 emissions
IMO2050

ABSTRACT

The International Maritime Organization aims to achieve full decarbonization by 2050 in response to climate change. This ambitious goal demands well-defined strategies guided by techno-economic assessments. The complexity of global shipping systems makes predicting long-term maritime trade patterns challenging, necessitating scenario-building rather than precise forecasts. Investigating shipping demand scenarios is crucial due to the uncertainty brought by the energy transition and its role as the primary driver of shipping emissions. This paper improves the representation of maritime shipping in Integrated Assessment Models (IAMs) by examining the impacts of climate targets on future shipping demand. A novel econometric model, grounded in advanced gravity theory and integrated with machine-learning algorithms, is proposed to estimate the elasticities of variables in bilateral seaborne trade. By coupling this model with the WITCH IAM, we explore various scenarios, providing deeper insights into trade patterns and their implications. The results show that stricter climate policies and higher carbon taxes reduce GDP due to higher abatement costs, higher fuel prices, and therefore reduced seaborne trade, especially for oil products and containerized cargo. Early adoption of carbon taxes in Europe may shift oil production and consumption patterns, temporarily boosting seaborne trade. Sub-Saharan Africa could experience significant demand growth due to economic and population increases.

1. Introduction

Our generation has to deal with the ongoing challenge of climate change. This is mainly due to greenhouse gas emissions, especially CO_2. The Paris Agreement aims to limit global warming to well below 2 °C, aiming to keep it under 1.5 °C (Agreement, 2015). Although the Agreement was unanimously accepted by the parties to the United Nations Framework Convention on Climate Change, it excludes major emitters from the international aviation and shipping sectors. According to Article 2.2 of the Kyoto Protocol, the International Maritime Organization (IMO) is tasked with regulating GHG emissions from international shipping (Hackmann, 2012).

The shipping sector is crucial in global trade, transporting over 80% of goods by volume and more than 70% by value. 94% of the world's fleet primarily handles this extensive activity, contributing significantly to greenhouse gas emissions (UNCTAD, 2021, 2022). Maritime shipping has accounted for CO_2 emissions of roughly 1.0 $GtCO_2$/yr in recent years (or 2.8% of global CO_2 emissions). Around 70% of this total originated from international shipping (IMO, 2020; International Energy Agency, 2024). As maritime shipping is inextricably linked to economic growth, sectoral emissions are expected to continue rising (Meersman and Van de Voorde, 2013; Serra et al., 2020; Naghash et al., 2024).

Over the past decades, the IMO has introduced several measures to enhance energy efficiency and reduce carbon intensity in the shipping sector. Notable initiatives include the Energy Efficiency Design Index (EEDI) for new ships, the Energy Efficiency Existing Ship Index (EEXI) for existing vessels, and the Ship Energy Efficiency Management Plan (SEEMP) alongside the Carbon Intensity Indicator (CII) to improve operational efficiency (Tokuşlu, 2020; DNV, 2022, 2021; IMO, 2020; International Maritime Organization, 2024). In 2023, the IMO revised its strategy, aiming for net-zero life-cycle GHG emissions around 2050 rather than 2100, including carbon dioxide removal (CDR) methods. This updated goal underscores the sector's commitment to global climate mitigation efforts (Comer and Carvalho, 2023). However, the pathways to achieving this target are still unclear and uncertain.

To comprehend emission reduction targets, it is crucial to understand the entire process chain that leads to emissions. Emissions from

☆ The research presented in this paper is part of the EU-funded Horizon 2020 project MAGPIE (sMArt Green Ports as Integrated Efficient multimodal hubs, contract No.: 101036594).

* Corresponding author.
E-mail addresses: H.Naghash@tudelft.nl (H. Naghash), D.L.Schott@tudelft.nl (D. Schott), J.F.J.Pruyn@tudelft.nl (J. Pruyn).
[1] Contributing Authors.

https://doi.org/10.1016/j.oceaneng.2025.120516
Received 3 October 2024; Received in revised form 15 January 2025; Accepted 23 January 2025
Available online 5 February 2025

maritime transport are closely tied to the composition of fuel supply, which depends on the demand for shipping activity. Also, recent fluctuations in the shipping market, such as COVID-19, have underscored the impact of this volatile demand (Merk et al., 2022). An even greater source of volatility is the energy transition. Efforts to reduce the carbon intensity of transport will likely increase costs due to carbon taxes or the adoption of more expensive technologies and designs. This introduces significant uncertainty for the future market and investors in the sector. Therefore, understanding the evolving demand for shipping activity is essential.

In response to this uncertainty, models are required. So far, sectoral models have been used extensively to explore the decarbonization of international shipping (Müller-Casseres et al., 2021). However, these models often treat shipping demand as an exogenous variable, failing to capture significant connections to other aspects of the global economy. This limitation is critical because the shipping sector links product flows across regions and sectors, making it sensitive to regional developments and policy changes. Moreover, technological improvements and the transition to alternative marine fuels are closely linked to similar advancements in other energy-using sectors (Raucci et al., 2023).

Integrated Assessment Models (IAMs) provide a valuable tool for addressing these limitations. IAMs have been extensively utilized to examine the consequences of different long-term climate mitigation strategies and have significantly impacted climate governance and policy. They offer a detailed representation of the world's energy, land use, agricultural, and climate systems, including interlinkages across sectors and regions over time. A common approach for exploring the future under complexity and uncertainty is developing a set of contrasting, plausible scenarios. These scenarios help understand how different factors interact, either working together or against each other, providing a systematic way to compare possible futures and guide climate policy-informed decisions (Walsh et al., 2019; Müller-Casseres et al., 2021, 2023; Speizer et al., 2024a).

However, IAMs also have notable gaps. Long-term scenarios developed by these models often pay relatively little attention to emissions from international transport, typically projecting shipping demand through aggregated relationships with income and without differentiating cargo types. Recently, the IAM community has started to incorporate the specificities of international shipping, improving the representation of the sector's demand and mitigation options within these models. Walsh et al. (2019) used the TIAM UCL model[2] to project the future of energy product trade, translating energy trade flows into tangible metrics like tonnes and aiding in analyzing interregional energy commodity trade under various scenarios. The goal is to optimize energy trade to maximize global welfare and minimize energy system costs. Müller-Casseres et al. (2021) used the IMAGE model,[3] where each region can import based on relative production and transportation costs, the latter depending on the distance. Fuel distribution from suppliers is determined using a multinomial logit equation, favoring the cheapest supplier. Also, Speizer et al. (2024b) used the GCAM model[4] to improve the representation of shipping activity by modeling it explicitly in terms of service, such as ton-kilometers, for both international and domestic shipping. GCAM scenarios incorporate reduced shipping demand driven by carbon pricing and economic factors, factoring in price elasticity and the effects of carbon policies on activity levels.

Despite notable improvements in these recent studies, IAMs typically categorize countries as either pure exporters or importers, especially for energy cargoes. This results in neglecting the complexities of cross-trading, where a region can be both an importer and exporter of a specific product. This is important because fuel supply and emissions are related to the actual physical transport rather than the macroeconomic energy balance or trade value in monetary terms. Additionally, most current models primarily rely on cost optimization for estimating energy trade. This approach does not adequately account for non-cost factors such as bilateral political or geographical specifics, which can significantly influence trade patterns. A recent multi-IAM shipping study (Müller-Casseres et al., 2023) has further emphasized this point, identifying the low representation of shipping activity as a key limitation across IAMs. Therefore, a coordinated effort to enhance shipping representations across multiple IAMs is required. In this paper, we aim to advance the representation of maritime shipping within IAMs, with a particular focus on the WITCH model. By leveraging the integrated framework, we incorporate macroeconomic drivers of shipping demand alongside detailed activity-based modeling. This enables us to produce more accurate projections and generate policy-relevant insights into the decarbonization of the maritime sector.

Building upon previous research, this paper introduces an econometric approach, an enhancement of the traditional gravity model of international trade, applied to various cargo types. Projections are made on bilateral trade flows calibrated on actual trade data, ensuring the capture of cross-trading effects. Subsequently, the econometric models are coupled with the WITCH IAM model (De Cian et al., 2009). For further policy analysis, this model is calibrated based on historical values and used to analyze the outcomes of multiple scenarios. Four distinct scenarios have been selected to assess the effects of mitigation efforts on seaborne shipping activity. They vary in their carbon tax scheme policies. The trade scenarios encompass nearly all seaborne traded commodities transported by dry bulk, wet bulk, and container vessels across 17 global regions.

This article is structured as follows: following this introduction, the methodology for econometric models, scenarios, and integration into the integrated assessment model is explained. Next, the results of the econometric analysis and the scenario runs are presented. Finally, we discuss the findings and their policy implications.

2. Methodology

Fig. 1 depicts the methods outlined in this section used to develop shipping activity scenarios, consisting of two main components: econometric analysis and coupling with the Integrated Assessment Model. The econometric analysis involves three main approaches tailored to different non-overlapping cargo categories, aiming to identify and quantify the impact of influential macroeconomic factors on regional and bilateral trade for each cargo type. The specific cargoes analyzed include oil and petroleum products, LNG, coal, iron ore, grains, containerized cargo, and minor bulks. These eight cargoes are grouped into three main modeling categories: *energy cargo*, *non-energy major bulk*, and *minor bulk & containerized cargo*. The reference for choosing this categorization of cargoes is the Clarkson Shipping Intelligence Network (SIN) list of cargoes, excluding the not significant ones such as chemicals and vehicle trades. Our selected range of cargo covers more than 90% of global seaborne trade. We use historical data to identify patterns and determine elasticities within these models. Each model's specifics differ in terms of estimation method and influencing variables, which will be discussed in detail in the next sections. Subsequently, these econometric models and the derived elasticities are integrated into the WITCH IAM for policy evaluation and scenario development. The analysis is long-term and global in scope.

The aim is to obtain the elasticity of change of each chosen determinant variable on the amount of trade. The primary outcome of the model is the quantity of each traded cargo from one region to another on a mass basis. Then, by considering proxy ports for each region, the average distance between regions is obtained, and thus, the amount of seaborne transport work (mass × distance) is estimated. Calibration occurs for each cargo against the real data of the 2020 total seaborne trade. This study prioritizes reflecting maritime transport

[2] Pye et al. (2020).
[3] Van Vuuren et al. (2015).
[4] Calvin et al. (2019).

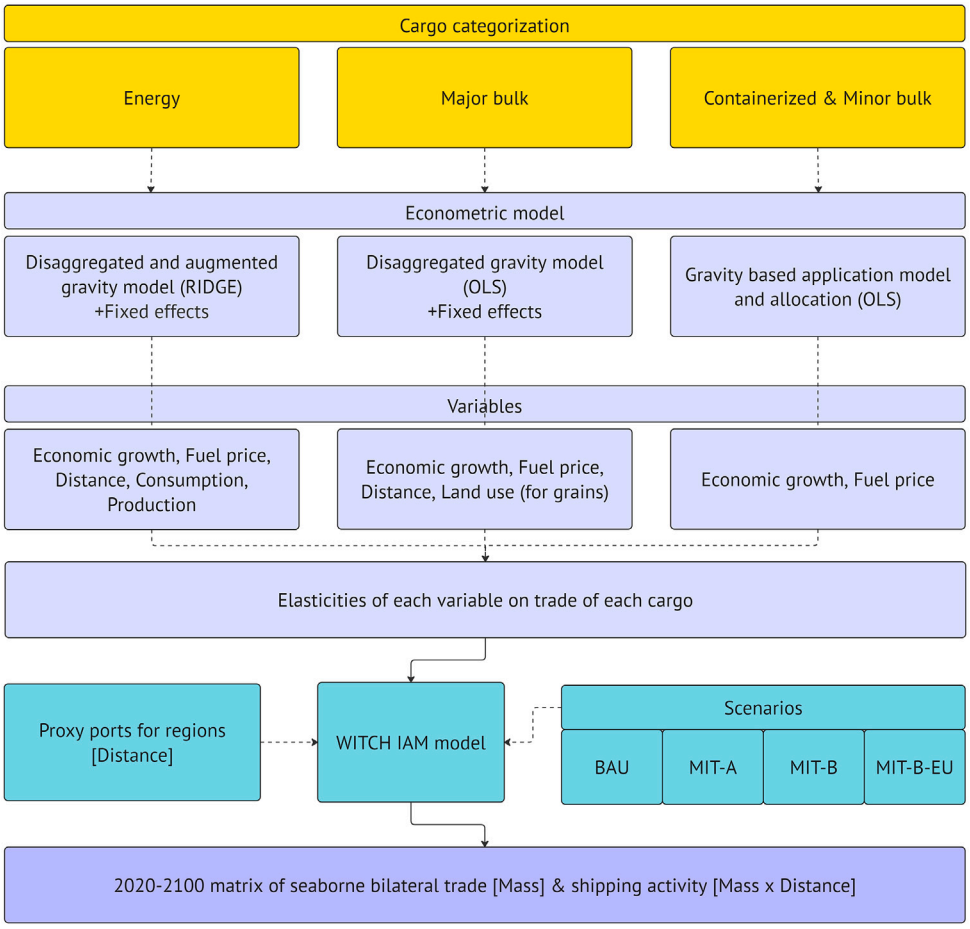

Fig. 1. Methodology framework.

work by focusing on the seaborne portion of trade flows. While adjacent regions like Russia–China, Russia-Europe, Canada-USA, and the Rest of South America-Brazil heavily rely on pipelines and land transport for oil and petroleum products, these flows were not excluded. Instead, their seaborne components were extracted explicitly for analysis.

2.1. Econometrics

While several theories explain international trade, such as comparative advantage (Do et al., 2016) and the Heckscher–Ohlin model (Leamer et al., 1995), the gravity model has emerged as the most commonly used framework (Zhang et al., 2015; De Benedictis and Taglioni, 2011). This model is based on the Armington assumption (Alston et al., 1990). The basic gravity equation states that the trade flow between countries depends primarily on the size of the economies and the distance between importer and exporter. This model can effectively depict bilateral trade patterns (Buongiorno, 2016; Zhang et al., 2018). Authors in Ubøe et al. (2009) concluded that cost-minimizing models provide relatively poor fits to observed behavior compared to a simple gravity model. The following expression shows the classical gravity model.

$$Trade(O, D) \propto \frac{GDP_{Origin}.GDP_{Destination}}{Distance} \quad (1)$$

Early applications of the gravity model in maritime contexts, such as analyzing seaborne coal and crude oil flows (Adland et al., 2017; Babri et al., 2017; Ubøe et al., 2009), primarily relied on including distance and national income as core predictors. Over time, these models evolved to accommodate more sophisticated features, such as country-specific fixed effects, energy structures, and political risks (Zhang et al., 2015, 2018), and to incorporate various trade-enhancing or inhibiting factors like colonial relationships and common language (Kottou et al., 2020). Furthermore, methodological extensions have emerged to improve predictive performance: gravity specifications have been combined with machine learning algorithms (Circlaeys et al., 2017; Sun et al., 2018; Kottou et al., 2020) and, more recently, graph autoencoders (Minakawa et al., 2022) to capture complex relationships in bilateral trade. In maritime-oriented studies, these enriched models effectively evaluate shifts in LNG trading patterns and forest product exports (Buongiorno, 2016; Zhang et al., 2018). Also, studies such as Tang et al. (2019), Chou et al. (2008) and Huang et al. (2018) used various types of gravity models to forecast and analyze container shipping trade flows.

The gravity model is typically used to estimate the value of trade rather than its physical mass when aggregated over total trade (De Benedictis and Taglioni, 2011). However, in this paper, we will break it down for each cargo category to increase accuracy and use it to determine the mass of trade. This is important because the mass of trade affects transport work and leads to emission estimation, unlike trade value. Our approach to modeling trade flows recognizes that a single model cannot fit all types of cargo, yet we strive to keep the methodology as straightforward as possible. Estimating bilateral trade for each cargo category is a key objective that drives our approach. For energy cargoes, we augment the gravity model with variables such as production and consumption of the commodity, as well as fuel prices, alongside the traditional factors of GDP and distance. This allows for a more precise analysis of trade patterns in the energy sector. A similar model is employed for non-energy major bulk commodities like grains and iron ore. In the bulk model, production and consumption data from the IAM are not used because they are themselves

derived from economic growth. To avoid double-counting GDP in both the production/consumption projections and trade projections, we rely solely on GDP for the projections. Thus, the model for bulk commodities includes GDP, distance, and fuel prices as the primary variables, while for grain, land use for agriculture is also incorporated to capture the critical economic drivers. To ensure the accuracy of these models, a Variance Inflation Factor (VIF) test is conducted to assess multicollinearity among variables, allowing us to use the appropriate estimation method for accurate coefficient estimation. For minor bulk and containerized cargoes, a different methodology is necessary due to the diverse nature of these goods and the challenge of finding detailed bilateral and quantity-based data. Each subcategory within these groups, such as specific manufactured products in containerized cargo or distinct types of minor bulk goods, often represents a smaller share of total trade, making standard methods less applicable. Specifically, traditional methods fall short for manufactured goods typically shipped in containers due to the lack of reliable historical data by region in terms of weight. Instead, historical data is often available only in product values. A distinct approach was developed for containerized cargo to address these challenges, treating it as a separate commodity category. The method for minor bulk differs from that for all previous categories due to more limited data, necessitating a more aggregated approach. Both aim to estimate bilateral trade flows while considering each cargo type's unique characteristics and data constraints. The analysis excludes other factors, such as environmental regulations, port infrastructure, common language, colonization, and political stability, as the focus is primarily on macroeconomic drivers and the impacts caused by climate policies.

2.1.1. Energy cargo

The gravity model serves as a valuable tool for predicting bilateral trade. However, its applicability in energy cargo remains limited, with few exceptions, such as Zhang et al. (2018) and Maxwell and Zhu (2011), who successfully utilized this model to estimate LNG trade flows. Additionally, Ubøe et al. (2009) employed the Gravity and cost-minimizing models to compare the results for predicting coal seaborne trade using distance and transportation costs. Similarly, Adland et al. (2017) applied the model to analyze crude oil exports using distance and supply & demand factors using AIS data. Babri et al. (2017) adapted the model to specialize in international trade flows of coal, iron ore, and crude oil, incorporating GDP, distance, and a fixed component to account for trade habits and contracts.

In this study, we will modify the gravity model and make it specialized for determining the bilateral trade of fossil fuel energy commodities: crude oil & petroleum products, natural gas, and coal. This is done by predicting variables and using a fixed-effect component. Adding more cargo-specific determinants increases the reliability of results. Fixed-effect controls the unobserved heterogeneity in data such as bilateral trade momentum and agreements (Buongiorno, 2016; Gómez-Herrera, 2013). To improve the estimation method and find the elasticities of change of each determinant, a log–log linearization is done to the equation (Silva and Tenreyro, 2006; Siliverstovs and Schumacher, 2009). The equation comes as follows:

$$\ln Trade_{OD,t} = \beta_0 + \beta_1 \ln V_1 + \beta_2 \ln V_2 + \cdots + \beta_n \ln V_n + \eta_{OD} \quad (2)$$

where $Trade_{OD,t}$ is bilateral trade flow, β_n is the elasticity of the determinant variable of V_n, and η_{OD} is the origin–destination fixed-effect components. The variables to include in the study are the GDP, production, and consumption of both importer and exporter regions and the average distance of shipping and fuel prices. The rationale behind choosing GDP is straightforward as it is a primary determinant of trade and a proxy of economic growth (Michail, 2020; Michail et al., 2021; Chou et al., 2008; Meersman and Van de Voorde, 2013). Distance and fuel price are proxies for transport costs (Zhang et al., 2015; Li et al., 2022). An escalation in the price of bunker fuel is expected to reduce trade volume, particularly for imports from distant regions. The interplay between production, consumption, and regional supply–demand dynamics significantly impacts global trade. For exporting countries, the availability of natural resources and their extraction/production directly influences their capacity and willingness to export. Higher reserves indicate a secure energy future, encouraging exports to increase revenue. Therefore, production levels are a key factor, representing the country's ability to supply the market. On the import side, When a country's domestic production falls short of its consumption needs, it must rely on imports to meet demand and ensure economic stability (Zhang et al., 2015, 2018; Maxwell and Zhu, 2011). Consumption and production of oil are crucial variables for both crude oil and petroleum products.

The empirical data used in this study was based on open-source data banks. BPstats (BP, 2021) was used as the main source of data for bilateral energy trade flow for 2014–2021. The data for sea trade was extracted, and marginal flows — less than 0.005 million tonnes — were excluded. The same reference is used also for regional production and consumption of energy sources. The World Bank was used to gather the GDP values of the regions (World Bank, 2024). All values are normalized based on 2005 USD to dampen the effect of inflation. The global average bunker price value is gathered from Clarkson Research Services (Han and Wang, 2021). After collecting all the data, they were organized to create a panel dataset containing every bilateral trade flow of each commodity. Zero flows have been removed from the dataset as suggested by Gómez-Herrera (2013) and Wohl and Kennedy (2018).

A variance inflation factor (VIF) test was performed to assess the presence of multicollinearity among the variables in the dataset. Substantial multicollinearity, indicated by a high VIF, suggests a variable is highly correlated with others, potentially leading to inflated standard errors and unreliable coefficient estimates in the regression model (Thompson et al., 2017). In this case, the RIDGE estimation method is recommended over ordinary least squares (OLS) (Kidwell and Brown, 1982). RIDGE introduces a penalty to the magnitude of coefficients, thereby reducing their variance and enhancing stability in the presence of correlated predictors. The presence of multicollinearity, as evidenced by VIF values higher than 5, calls for adopting the RIDGE method. The table of VIF values is presented in the Appendix. Also, the dataset is divided into two parts: 80% for the train and 20% for the test. To increase the reliability of the results, k-fold cross-validation is implemented.

2.1.2. Major bulk cargo

The primary cargoes examined in this section are whole cereals, including wheat, rye, barley, oats, maize (corn), rice, grain sorghum, and iron ore (and concentrates, including roasted iron pyrites).[5] Historical bilateral trade data obtained from Trade Map (Trade Map, 2024) (2015–2021) are used in econometric models to measure trade elasticities for each commodity. The analysis uses bilateral data, including the GDP of both exporting and importing regions, distance, fuel prices, and, for grains specifically, the area of exporters' agricultural land use,[6] to estimate trade flows by region and commodity, using 2020 as the baseline year. A fixed effect component is included to account for the bilateral trade momentum.

Similar to the approach for energy cargo, the dataset is divided into a training set (80%) and a test set (20%), with k-fold cross-validation implemented to enhance the reliability of the results. The general approach remains consistent, as the production and consumption of these commodities are also generally influenced by GDP. Including GDP as a determinant variable in the models prevents redundancy while addressing the key factors driving trade flows. The primary differences lie in the specific variables selected and the estimation methods used, guided by the results of the VIF test. The OLS estimation method is used here because multicollinearity does not exist in these datasets.

[5] The HS code for iron ore is 2601, and for grains, it ranges from 1001 to 1008.

[6] Food and Agriculture Organization of the United Nations (2024).

2.1.3. Minor bulk & containerized cargo

This study utilizes econometric models to estimate bilateral trade flows of containerized cargo, using data from Clarkson's SIN database (Clarkson Research Services, 2024) covering regional exports and imports from 2002 to 2021, supplemented with regional GDP figures and global average fuel prices for each year. We employed OLS regression to quantify the coefficients of trade flows to GDP and fuel prices, represented by coefficients (betas). The core equation includes a general trade model, which predicts trade volumes using GDP and fuel prices, and another function that distributes the trade among regions to form bilateral trade. Specifically, the general trade equation models the relationship between trade (imports or exports), GDP, and fuel prices, while the bilateral trade equation calculates the trade volume between an origin and destination region over time, factoring in the proportional allocation of trade.

$$Trade_{X/I}(t, O/D) = \beta 0_{I/X} \times GDP^{\beta 1_{X/I}} \times fprice^{\beta 2_{X/I}} \tag{3}$$

$$Trade_{OD,t} = Import_D(t_0) \times \exp\left(\beta 1_I \cdot \ln\left(\frac{GDP_D(t)}{GDP_D(t_0)}\right) + \beta 2_I \cdot \ln\left(\frac{fprice(t)}{fprice(t_0)}\right)\right) \times \frac{Allocation_O(t)}{\sum_O Allocation_O(t)} \tag{4}$$

$$Allocation_O(t) = \beta 0_X \times GDP^{\beta 1_X}(t) \times fprice^{\beta 2_X}(t) \tag{5}$$

The trade equation for modeling containerized cargo flows consists of three main multiplicative components. The first component, $Import_D(t_0)$, represents the base-year import volume at the destination. The second component predicts the import growth by considering the GDP and fuel price change from the base year t_0 to the current year t. The coefficient β_1 represents the elasticity of trade flow to GDP, and β_2 represents the elasticity to fuel price. The third component, $\frac{Allocation_O(t)}{\sum_O Allocation_O(t)}$, allocates the predicted import volume to various exporting regions based on economic factors at the origin. In this term, $Allocation_O(t)$ is a function of the origin's GDP and fuel price, capturing the proportion of total imports attributed to each origin. Together, these components provide the model for estimating containerized cargo trade flows, incorporating base-year data, growth predictions, and import allocation among exporting regions.

Regarding the minor bulk, time-series data of total global trade are available (Clarkson Research Services, 2024). A similar equation as containerized cargo applies to this category as well. Afterward, bilateral trade is allocated based on the economic growth of each region at each time step. The approach is quite similar to containerized cargo, with the difference in the non-differentiating regional coefficients due to a lack of data.

2.1.4. Models' validation

The econometric models were validated using recently released data from 2022 and 2023. Initially trained on data up to 2021, the models were tested against this holdout set to assess their predictive performance. This approach ensures the models can generalize to new observations, reflecting their applicability in dynamic trade environments. Validation metrics, including R-squared (R^2), mean squared error (MSE), root mean squared error (RMSE), and mean absolute error (MAE), were computed to evaluate the models' predictive accuracy. Additionally, actual versus predicted trade values were plotted for visual inspection. The validation results demonstrate strong performance across all model categories, with high R^2 values and minimal errors observed in key metrics. The models successfully captured trade dynamics across diverse cargo types. For further validation, this study includes a comparison with similar works that predict global shipping demand. Validation plots and a metrics table are provided in Appendix A.3.

2.2. Coupling with the integrated framework

After creating models for each cargo type and estimating each predictive variable's impact on bilateral trade, the models are integrated into an Integrated Assessment Model to develop scenarios and evaluate policies. The following sections provide a detailed explanation of the IAM framework and the scenarios.

2.2.1. Integrated Assessment Model (IAM)

IAMs describe key processes in the interaction of human development and the natural environment. Typically, they are designed to assess the implications of achieving climate objectives, such as limiting global warming to 2° or 1.5° (Müller-Casseres et al., 2023; Riahi et al., 2021; Weyant, 2017). These models are crucial for exploring future climate actions and informing policy decisions (Van Beek et al., 2020). IMO relies on these models for future projections of the sector.

This study employs the WITCH IAM, a renowned model featured in the IPCC Assessment Reports (Mastrandrea et al., 2011; Byers et al., 2022). The model integrates a hybrid structure that combines top-down macroeconomic intertemporal optimization with bottom-up technological insights into the energy sector. It emphasizes optimal mitigation and adaptation strategies for climate change, accounting for regional welfare, free-riding behaviors, and externalities. A social planner approach maximizes regional utility, considering fossil fuel and GHG mitigation costs. A key strength lies in its detailed representation of energy and economic sectors. However, the international shipping module was in its early stages and highly aggregated (Müller-Casseres et al., 2023). The model operates with a time horizon extending to 2100 and utilizes intertemporal optimization with perfect foresight. It adopts a general equilibrium solution concept and applies a flexible discount rate based on the Ramsey rate, typically ranging from 3.0 to 5.0 percent per year. The current version, WITCH 5.0, encompasses 17 regions defined by geographic, income, and energy demand characteristics. Fossil fuel extraction is handled by requiring a capital investment for production, which depreciates over time. Costs increase with resource depletion, with different oil grades having varying costs and emissions. The model uses fossil fuel availability curves for coal and gas extraction, aligning production with international prices and market demand. Further technical details are available in the WITCH 5.0 Documentation (WITCH Model Development Team, 2024; Integrated Assessment Modeling Consortium (IAMC), 2024).

2.2.2. Ports and distances

To approximate the distances involved in international trade, we identified the largest ports in each region as proxy ports; for Sub-Saharan Africa, the USA, and Canada, both east and west coast ports were used to capture diverse shipping routes. Sea distances between these ports were obtained from an online tool (Sea Distances, 2024), which provides multiple route options—ranging from shortest to longest. The routes pass through chokepoints such as the Panama Canal and Suez Canal, subject to ship-size limits, and through passages such as Cape Horn and the Cape of Good Hope, which impose no vessel-size constraints. The permissible vessel sizes for each route were extracted and matched with the proportions of different vessel types, as reported in the IMO's 4th GHG study, along with corresponding cargo categories. A weighted average distance was then calculated based on the shortest feasible route for each ship-size class and cargo type, ensuring that the respective size limitations and vessel shares were accounted for. More data used to form the spatial matrix of distances, and sources are provided in the Appendix A.2. An illustrative example is the route between Europe's Port of Rotterdam and Japan's Port of Chiba; where the shortest distance (11,195 nautical miles) is via the Suez Canal, but oil tankers larger than Suezmax (i.e., ULCC or VLCC) must travel via the Cape of Good Hope, which extends the route to 14,511 nautical miles. Since 61% of tanker capacities can still pass through the Suez Canal, the weighted average distance is calculated as:

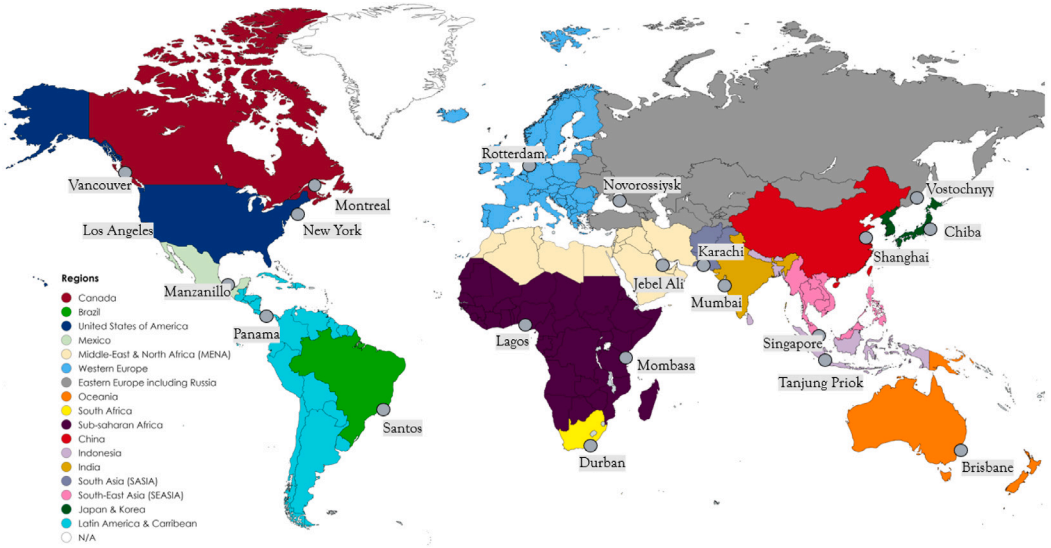

Fig. 2. Representative regions and proxy ports.

$$Avg.Distance : [0.61 \times 11195 + 0.39 \times 14511] = 12488 \text{ nautical miles}$$

Although this approach involves rough assumptions, it provides a sufficiently accurate estimate, as the primary need is for an average distance. A calibration process will subsequently align these estimates with actual 2020 shipping data. Fig. 2 shows the regions and proxy ports for each region. Route and port traffic congestion is neglected in this study.

2.2.3. Scenario selection

The shared socioeconomic pathways (SSPs) are scenarios designed to depict global socioeconomic developments throughout the 21st century. The climate change research community created these scenarios to provide a unified framework for analyzing long-term climate impacts, vulnerabilities, and strategies for adaptation and mitigation (Riahi et al., 2017; O'Neill et al., 2017; Samir and Lutz, 2017). SSP2, or middle-of-the-road, is used as the baseline of scenarios. In the SSP2 narrative, a sort of midpoint between the other SSPs, socioeconomic indicators progress compatibly with historical trends, and there are no major technological disruptions (Fricko et al., 2017). The key distinction between the scenarios lies in the portfolio of the global carbon tax. In the non-MIT scenario, no carbon tax is implemented. So, the global tendency is to continue using fossil fuels and invest less in renewable energy. In this scenario, the average global surface temperature increases by 3.5° by the end of the 21st century. In scenario MIT-A, a uniform carbon tax is implemented to align with a 2° global temperature increase. Meanwhile, scenario MIT-B portrays a more rigorous carbon policy to limit the temperature increase to 1.5°. The MIT-B-EU scenario mirrors MIT-B, with the notable difference being that Europe adopted carbon tax two decades earlier than other regions. The details of the scenarios are presented in a Table A.11 and Fig. A.19 in the Appendix A.4.

3. Econometrics results

3.1. Energy cargo

The Table 1 presents elasticity estimates and model performance for coal, LNG, and oil products, focusing on the drivers of seaborne trade. Production is the most influential factor for coal trade in the exporting country, with a positive elasticity of (0.619), while distance has a significant negative impact (−0.287). LNG shows similar dynamics, with a robust positive elasticity for production in the exporter country (0.807) and a significant negative effect from distance (−0.589). In oil products, the key drivers are production in the exporter country (0.426) and consumption in the importer country (0.453). Only for oil and oil products is the elasticity of exporter consumption positive, as the transformation of crude oil into petroleum products is recorded as crude oil consumption in the data, even though it reflects petroleum product production. Price negatively impacts all cargoes, and GDP elasticities vary depending on whether they apply to exporters or importers. The model performs well, with R^2 scores ranging from 0.802 for coal to 0.949 for oil products, indicating robust predictive accuracy. These results emphasize that production and distance are the main determinants of energy trade, with varying degrees of sensitivity across different cargoes.

3.2. Major bulk cargo

The Table 2 presents the effects of various factors on the grain and iron trade. Grain imports are highly sensitive to the GDP of importing countries (elasticity 0.259), while distance negatively affects trade (−0.197), and the exporter's GDP has less impact. In iron trade, the exporter's GDP is the dominant factor (0.474), while the importer's GDP and distance play a more minor role. The models perform well, with high R^2 scores of 0.902 for grain and 0.941 for iron and low error metrics, indicating predictive solid accuracy.

3.3. Minor bulk & containerized cargo

The Table 3 displays coefficients ($\beta_0, \beta_1, \beta_2$) for the import and export of each region. It also shows the model performance metrics for containerized cargo trade across different regions. The elasticity values indicate how sensitive trade volumes are to changes in price and GDP. Economic growth in all importing and exporting regions substantially impacts trade volumes, with the highest impact observed in Europe and MENA. On the other hand, the price elasticity for most imports and exports is negative, indicating that higher prices reduce import volumes. The R^2 values range from 0.822 to 0.991, showing the models' strong ability to explain variations in trade volume. The performance metrics further confirm the models' good fit and accuracy.

Regarding the minor bulk, log–log multiple regression results revealed that a 1% increase in GDP is associated with a 0.83% rise in trade, while a 1% increase in fuel price results in a 0.15% decrease in trade. The model has high explanatory power (R^2 = 0.97) and

Table 1
Elasticity estimates and model performance for energy cargoes.

	Coal	Coal Std. Dev	LNG	LNG Std. Dev	Oil products	Oil products Std. Dev
Elasticities						
Production exporter	0.619	(0.075)	0.807	(0.045)	0.426	(0.024)
Consumption importer	0.300	(0.015)	0.429	(0.020)	0.453	(0.030)
Production importer	−0.092	(0.012)	−0.301	(0.016)	−0.006	(0.010)
Consumption exporter	−0.335	(0.084)	−0.541	(0.038)	0.154	(0.022)
Fprice	−0.322	(0.083)	−0.030	(0.009)	−0.036	(0.008)
Distance	−0.287	(0.019)	−0.589	(0.015)	−0.709	(0.013)
GDP importer	0.219	(0.047)	0.375	(0.022)	0.258	(0.037)
GDP exporter	−0.329	(0.039)	−0.063	(0.029)	−0.174	(0.046)
Metrics						
Average R2 score	0.802	(0.088)	0.819	(0.088)	0.949	(0.012)
Average RMSE	0.500	(0.113)	0.428	(0.113)	0.322	(0.033)
Average MSE	0.263	(0.128)	0.184	(0.128)	0.105	(0.021)
Average MAE	0.402	(0.077)	0.308	(0.077)	0.256	(0.025)

Table 2
Elasticity estimates and model performance for grain and iron.

	Grain	Grain Std. Dev	Iron	Iron Std. Dev
Elasticities				
GDP exporter	0.148	(0.006)	0.474	(0.050)
GDP importer	0.259	(0.008)	0.177	(0.114)
Distance	−0.197	(0.012)	−0.168	(0.019)
Fprice	−0.089	(0.018)	−0.103	(0.013)
Agricultural land-use exporter	0.149	(0.007)	–	–
Metrics				
Average R2 score	0.902	(0.008)	0.941	(0.007)
Average RMSE	0.257	(0.026)	0.272	(0.026)
Average MSE	0.067	(0.013)	0.075	(0.014)
Average MAE	0.151	(0.013)	0.145	(0.012)

accurately predicts trade values with low errors (MAE = 0.03, RMSE = 0.043). Due to a lack of detailed data, the estimated elasticities are global and aggregated over all regions for this category.

4. Scenario results and discussion

4.1. Future of international shipping demand

Global seaborne trade is projected to grow throughout the century, with the extent of growth heavily influenced by carbon policies. Shipping activity demands are expected to grow by 34%–66% by mid-century, with 2020 as the base year. In the non-MIT scenario, which lacks carbon regulations, trade could exceed 150 trillion ton-miles per year by 2100. In contrast, the MIT-A scenario, aligned with limiting global temperature rise to 2 °C, shows moderated growth, reaching around 125 trillion ton-miles. The MIT-B scenario, targeting a 1.5-degree limit, leads to even slower growth, just over 100 trillion ton-miles, driven by strict carbon regulations that reduce fossil fuels trade while boosting cleaner energy sources. In the MIT-B-EU scenario, where Europe enforces carbon taxes earlier, trade growth initially surpasses even the non-MIT scenario due to shifts in trade flows, which is explained later. However, it converged with the MIT-B results after the mid-century, reaching slightly below 100 trillion ton-miles.

Fig. 3 shows the amount of projected aggregated seaborne trade in mass and transport work in four scenarios. Fig. 4 shows the same but indexed and disaggregated by different cargo.

4.2. Trade in energy cargo

The non-MIT scenario projects the highest trade of fossil fuel energy commodities due to the absence of carbon policies. In this scenario, traditional exporters, such as the Middle East and the USA, maintain their dominance throughout the century, with stable trade patterns reflecting continued reliance on fossil fuels.

Interestingly, in the early years of the MIT-B-EU scenario, where only Europe enforces a carbon tax, there is initially higher trade in oil products compared to the non-MIT scenario. This paradox arises because Europe's carbon tax reduces domestic oil consumption, causing an excess supply that lowers global oil prices. Lower prices make oil more affordable for countries without carbon taxes, boosting their consumption. Additionally, reduced European demand shifts the investments to non-taxed regions, enhancing their oil production. As a result, global oil consumption and extraction initially rose despite Europe's reduced usage, driven by increased demand and production in regions without carbon taxes. However, as other regions implement carbon taxes, global trade patterns shift towards convergence with the MIT-B scenario, characterized by reduced fossil fuel trade and increased diversification of energy sources.

As shown in Fig. 5, there is a marked divergence in trade route trends for oil products depending on the scenario. Major routes such as MENA (Middle East and North Africa) to India and Seasia show a steady increase in trade volumes under the non-MIT scenario before it reaches a plateau, suggesting sustained demand for oil in these regions. In contrast, trade volumes along these routes decline sharply under the MIT-B and MIT-B-EU scenarios. China imports are peaking around 2045 and then declining, while in the MIT scenarios, the peak happens even sooner. These indicate that stricter climate policies could significantly reduce oil demand, particularly in Asia, where energy policies may shift away from fossil fuels. The most influenced routes through these scenarios are MENA-India, TE-Europe, and MENA-Seasia. Additionally, the MENA to SSA (Sub-Saharan Africa) route shows an upward trend across all scenarios, with a spike in the non-MIT scenario, highlighting SSA's growing role as a significant oil importer due to increased industrial activity and energy consumption.

In Fig. 6, LNG trade routes reveal stable or shifting patterns depending on the region and scenario. Routes such as MENA to India and MENA to Europe display significant growth in trade volumes under the non-MIT scenario, indicating higher future demand for natural gas as a transitional energy source. However, under the MIT-B and MIT-B-EU scenarios, trade volumes along these routes will stabilize or decline slightly by 2050, suggesting a shift towards renewable energy sources and reduced reliance on natural gas. This trend is particularly evident in the MENA to Europe route, where trade volumes decrease under stricter scenarios, indicating potential changes in Europe's energy import strategies and consumption patterns. Some routes, such as MENA to Jpnkor, trend upward or downward depending on the scenario, reflecting the variability caused by carbon policies. The most influenced routes through these scenarios are MENA-Europe and MENA-China.

Coal trade flows show a clear and consistent decline across all scenarios, with the steepest drops occurring under the MIT-B and MIT-B-EU scenarios. The competitiveness of alternative sources primarily drives the decline in coal consumption and production for energy

Table 3
Elasticity estimates and model performance for containerized cargo by region and trade direction.

Region	Trade direction	Constant	Price elasticity	GDP elasticity	R^2	MSE	MAE
Oceania	Import	2.201	−0.327	0.882	**0.956**	0.003	0.050
	Export	1.323	−0.211	0.597	**0.956**	0.002	0.033
North America	Import	0.894	−0.064	0.865	**0.864**	0.005	0.056
	Export	0.340	0.168	0.554	**0.886**	0.003	0.042
MENA[a]	Import	1.817	−0.350	1.233	**0.991**	0.001	0.034
	Export	1.194	−0.429	1.210	**0.950**	0.007	0.071
LACA[b]	Import	1.197	−0.252	0.910	**0.902**	0.007	0.061
	Export	1.529	−0.250	0.613	**0.663**	0.011	0.091
Indian sub-continent	Import	1.313	−0.056	0.831	**0.986**	0.003	0.038
	Export	0.966	−0.008	0.692	**0.986**	0.002	0.031
Far-East	Import	1.802	−0.063	0.865	**0.979**	0.003	0.042
	Export	2.159	−0.039	0.822	**0.962**	0.004	0.053
Europe	Import	0.017	−0.196	1.595	**0.892**	0.006	0.066
	Export	1.737	−0.135	1.678	**0.760**	0.014	0.102
Africa	Import	2.484	−0.379	1.327	**0.947**	0.009	0.082
	Export	0.966	−0.036	0.391	**0.910**	0.002	0.034

[a] Middle East and North Africa.
[b] Latin America and the Caribbean.

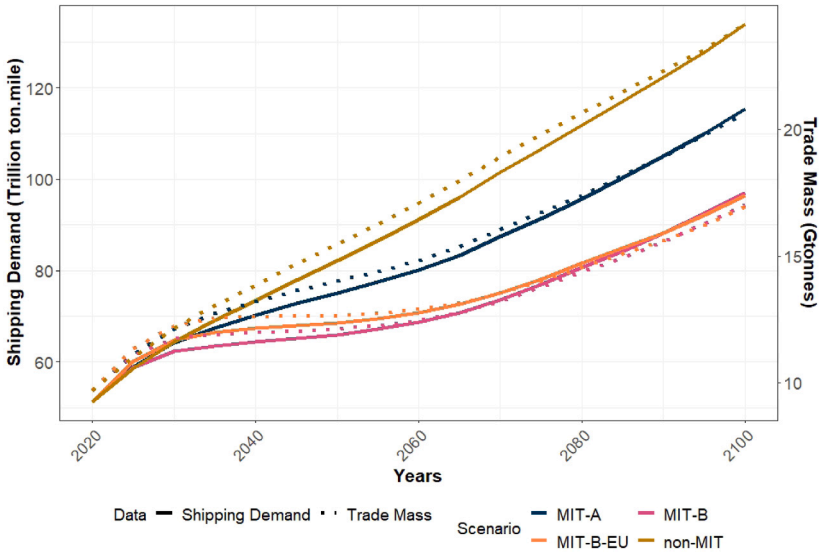

Fig. 3. Aggregated global sea trade of four scenarios.

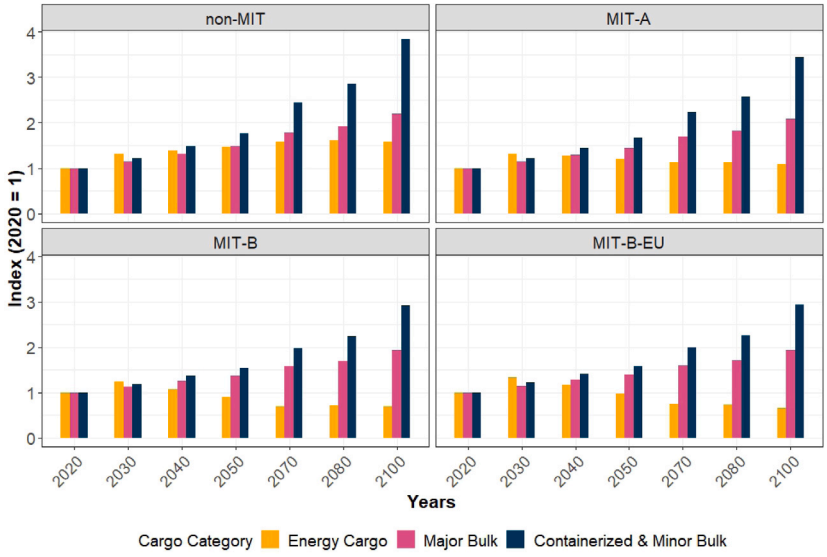

Fig. 4. Global sea trade growth of four scenarios by cargo categories.

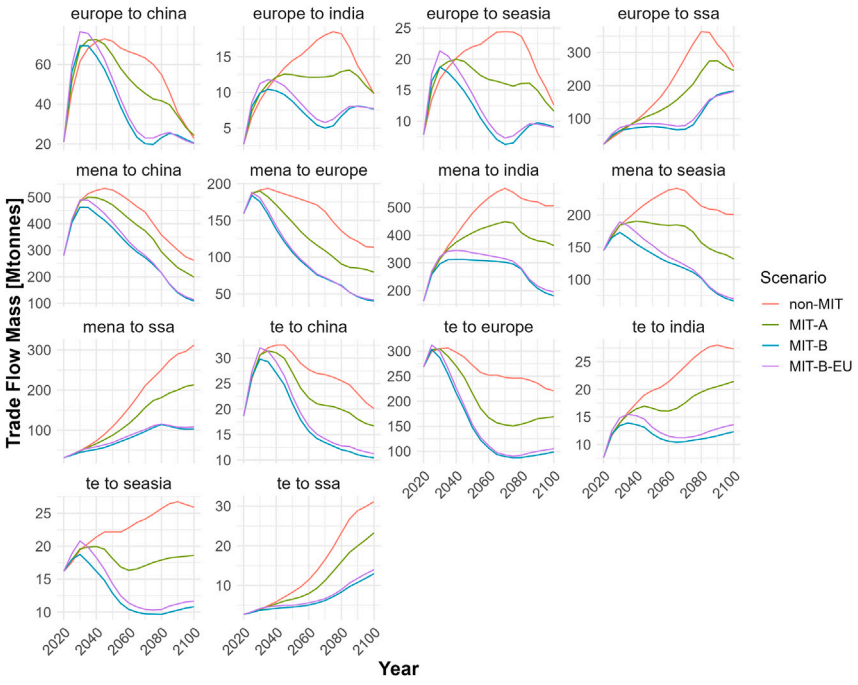

Fig. 5. Major sea routes of oil & products trade shifts over time and scenarios.

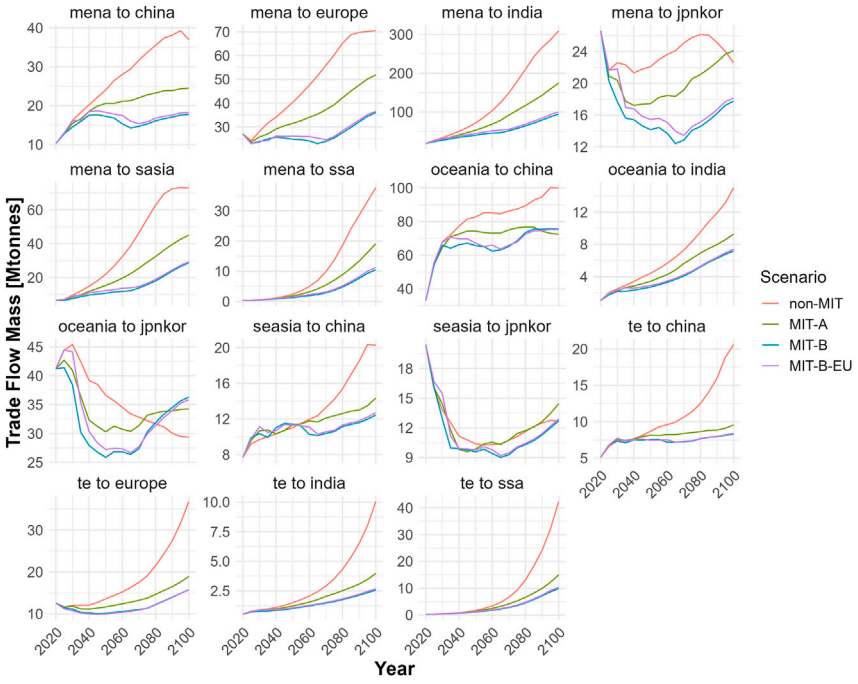

Fig. 6. Major sea routes of LNG trade shifts over time and scenarios.

generation. Renewable energy has become cost-competitive, decreasing coal demand, particularly in advanced economies. It is expected that global coal demand will continue to fall. Additionally, The aging coal infrastructure further increases the cost of coal, making investments in renewables or natural gas more attractive. These factors contribute to a sustained decrease in coal usage even under current measures without requiring stricter climate policies (International Energy Agency, 2023). Also, in all scenarios of the IPCC 6th report, Achakulwisut et al. (2023) compiled all coal projections and concluded that the global coal supply will rapidly decline, with coal use without CCS largely phased out entirely by 2040.

According to Fig. 7, key routes, such as Indonesia to China and Indonesia to Japan and Korea, exhibit a sharp reduction in trade quantity, reflecting a global move away from coal in favor of cleaner energy sources. Exports from Oceania are also significantly affected, similar to Indonesia, as demand for coal diminishes. In the non-MIT

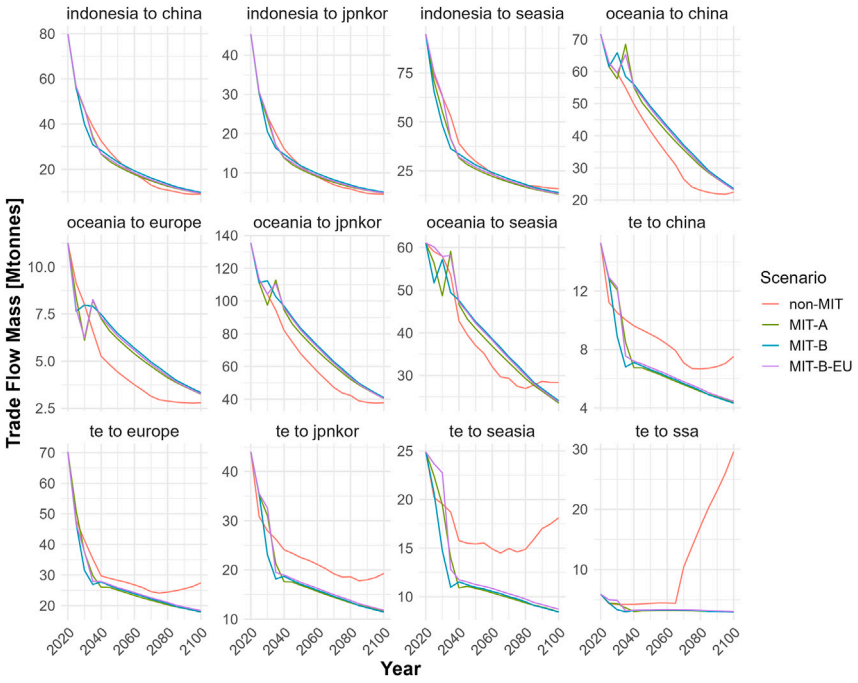

Fig. 7. Major sea routes of coal trade shifts over time and scenarios.

scenario, trade of routes involving Oceania exports is lower compared to the MIT scenarios. This is because the importer's reduced coal consumption has a more significant impact on the MIT scenarios. The most influenced routes through these scenarios are TE-Seasia and TE-Jpnkor. An interesting point is the upward trend of exports from TE to SSA after 2060 in the non-MIT scenario, driven by high consumption and growth in SSA. This is not happening in MIT scenarios, as the region's demand is satisfied by cleaner energy sources.

4.3. Trade in major bulk cargo

Iron ore and grains trade is projected to increase steadily as population growth and economic expansion drive higher demand. However, in mitigated scenarios with stricter carbon policies, the growth rate is slightly lower due to higher average fuel prices and higher abatement costs, which raise transportation costs and represent the economic cost of climate mitigation. The results show that grains and iron ore trade are less sensitive to climate policies and more driven by the combined effects of population and economic development. By 2100, shipping demand for grains is expected to remain between 9 and 11 trillion ton-miles, while iron ore demand is projected to stay between 20 and 24 trillion ton-miles. The divergence of scenarios usually starts to build up after around 2040.

Grain main trade routes in Fig. 8 show significant increases in trade volumes, particularly to Sub-Saharan Africa and MENA. For example, the Europe to SSA route demonstrates continuous growth under all scenarios, with the highest increases observed in the non-MIT scenario. This trend reflects rising food import needs driven by population growth and economic development. Similarly, grain trade volumes to MENA increase steadily, highlighting the region's dependency on grain imports to meet food security requirements. Notably, some routes, such as USA to JPNKOR under the MIT-B-EU scenario, show higher trade volumes, even slightly surpassing the non-MIT scenario, due to the lower global fuel prices explained earlier. The relatively uniform growth across scenarios suggests that grain trade is influenced mainly by demographic and economic factors rather than climate policy alone. The most influenced routes through these scenarios are TE-MENA and TE-SSA.

As shown in Fig. 9, Iron ore trade remains robust across all scenarios, particularly on major routes such as Oceania to China. The trade volumes on this route increase steadily, even under the MIT-B and MIT-B-EU scenarios, although the growth rate is more moderated than in the non-MIT scenario. This suggests that demand for iron ore, driven by infrastructure development and construction in regions like China, remains strong despite potential shifts towards sustainability and environmental regulation. The most influenced routes are Oceania-China and Brazil–China, reflecting their significant roles in meeting China's iron ore demand.

4.4. Trade in containerized cargo and minor bulk

Minor bulk and containerized cargo are projected to increase steadily and faster than other types of cargo due to their strong dependence on economic growth and population expansion. By 2100, the demand for containerized cargo is expected to range between 35 and 45 trillion ton-miles, while the demand for minor bulk is projected to be between 23 and 30 trillion ton-miles. This reflects their heightened sensitivity to economic activity and the overall expansion of the global economy.

In Fig. 10, trade routes for containerized goods consistently show strong growth across all scenarios, particularly routes to Sub-Saharan Africa. For instance, the Europe to SSA route experiences a continuous rise in trade volumes, reflecting SSA's expanding economic integration and increasing demand for consumer goods and manufactured products. Despite stringent climate policies like MIT-B and MIT-B-EU, these routes demonstrate upward trends, although the growth rate is slightly lower than in the non-MIT scenario. Interestingly, routes such as China-USA and Jpnkor-China peak around 2050–2060 and then decline, with the peak occurring sooner under the MIT scenarios. The Jpnkor-USA route is the only route showing a general decline across all scenarios. The most influenced routes through these scenarios are those where SSA is an importer as well as the China-Europe route. The robust growth in containerized goods trade to SSA and other emerging markets suggests a shift in global trade hubs and a move towards more diversified trade networks driven by economic growth and infrastructure development in these regions.

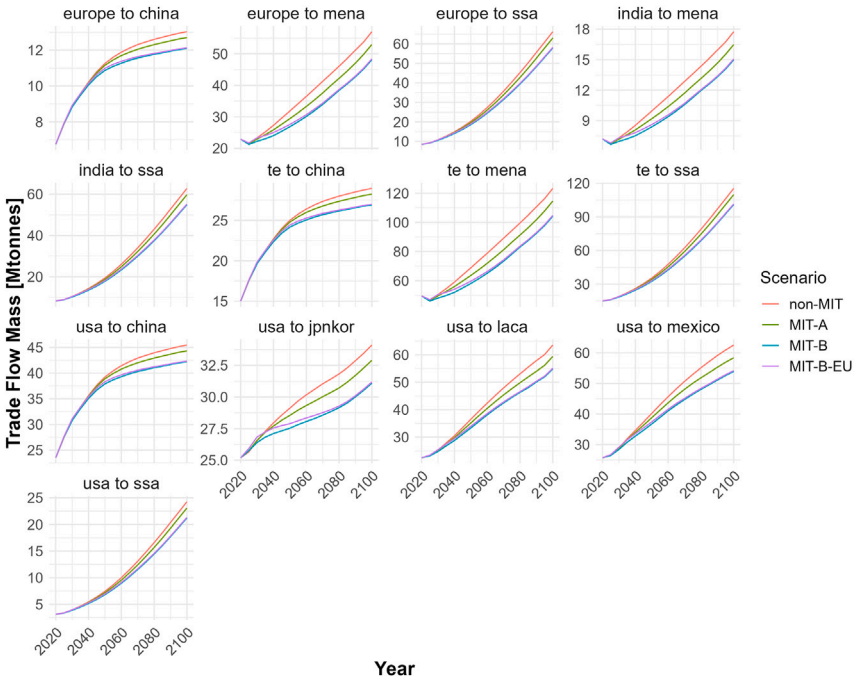

Fig. 8. Major sea routes of whole grains trade shifts over time and scenarios.

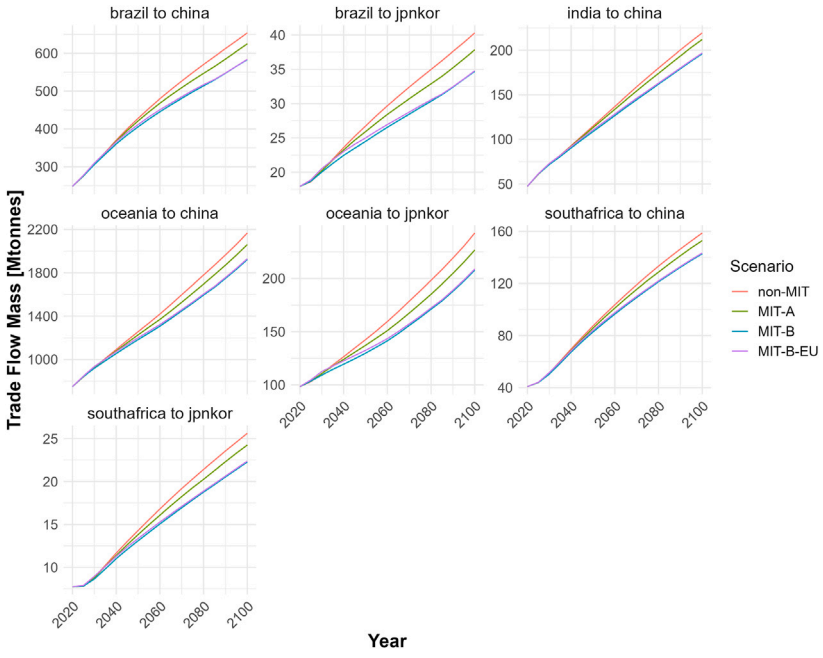

Fig. 9. Major sea routes of iron ore trade shifts over time and scenarios.

Illustrated by Fig. 11, Trade flows for minor bulks, which include a variety of bulk goods, depending on the scenarios. Regarding the shifting patterns, the China-Jpnkor route peaks around 2050 and then declines, with the peak occurring sooner under the MIT scenarios. A similar pattern is observed for the China-USA and Jpnkor-China routes. Some routes, such as SSA-Europe and SSA-USA, show sharp increases that are almost inelastic to the scenarios. Other routes' behavior entirely depends on the scenario, such as Europe-USA and USA-Europe, which decline in the MIT-B and MIT-B-EU scenarios but increase in the non-MIT and MIT-A scenarios. The most influenced routes are China-Jpnkor, both ways around, reflecting their significant role in minor bulk trade flows. The overall trends remain consistently upward across scenarios.

4.5. Discussion

- **Stricter carbon policies and higher carbon taxes are projected to reduce global seaborne trade** mainly due to mitigation-related economic loss and shifting fossil fuel production and consumption patterns. This decrease in trade is particularly significant for fossil fuel cargoes. These trends highlight the importance of cautious investment strategies for port infrastructure. Specifically, facilities heavily reliant on fossil fuel cargoes should plan for reduced volumes while opportunities may arise to adapt

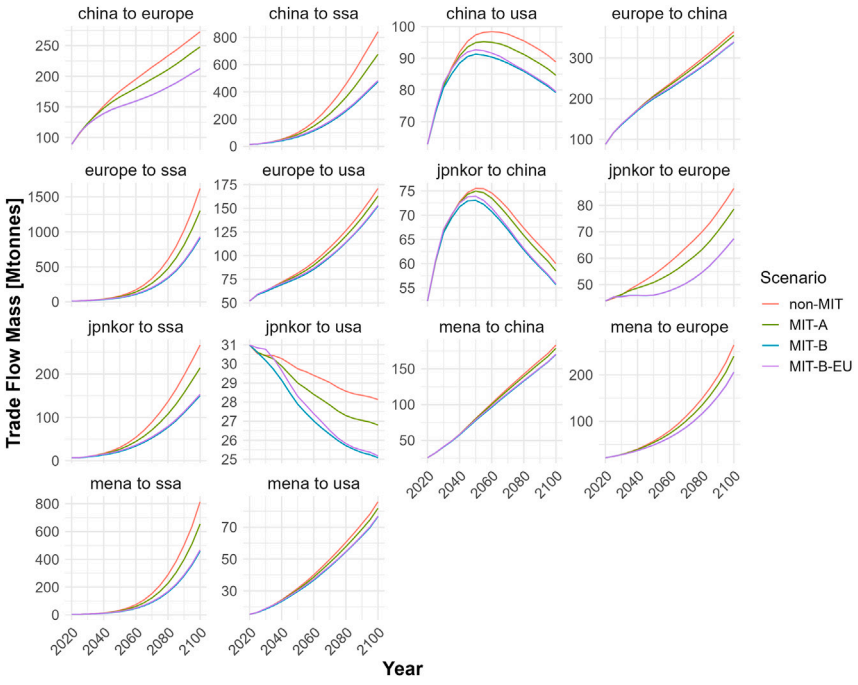

Fig. 10. Major sea routes of containerized trade shifts over time and scenarios.

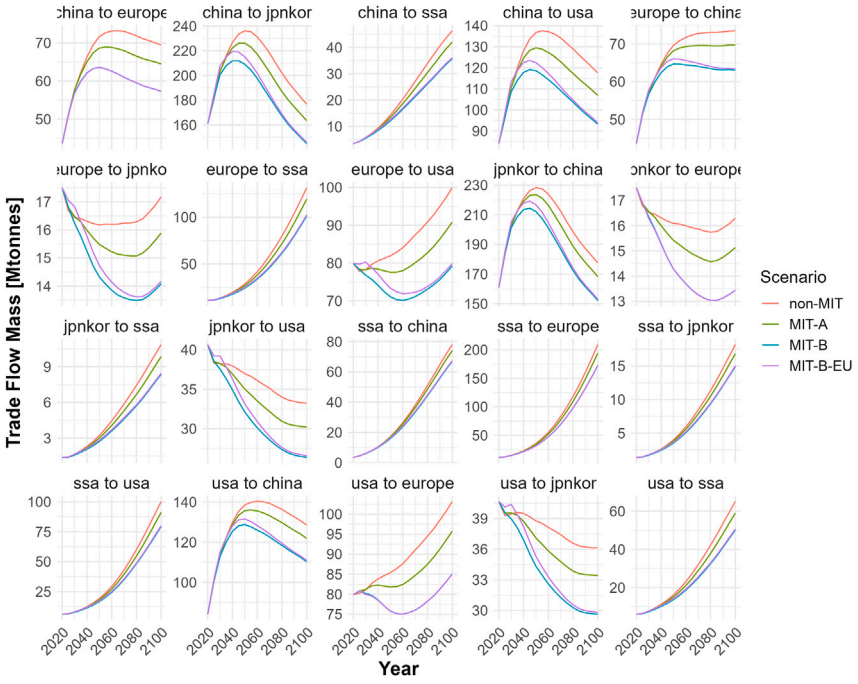

Fig. 11. Major sea routes of minor bulk trade shifts over time and scenarios.

infrastructure for cleaner energy products and resilient trade flows in non-energy sectors.

- **The total trade share of different cargoes is expected to shift**, with oil products, containerized cargo, minor bulk, and iron ore dominating by end-century across all scenarios. The trade of minor bulk goods and iron ore remains less sensitive to climate policies and is driven more by economic activity and manufacturing needs. Stakeholders should monitor these trends and invest in adaptable logistics and handling facilities to accommodate traditional and emerging cargoes. Shipowners might consider diversifying their fleets to include vessels capable of transporting various cargo types [Fig. 12]. There is potential for new trade markets, such as biomass and hydrogen, to emerge, although these are not explicitly covered in this study.
- **If Europe implements a carbon tax before other regions, it is expected to increase the seaborne trade, especially oil**

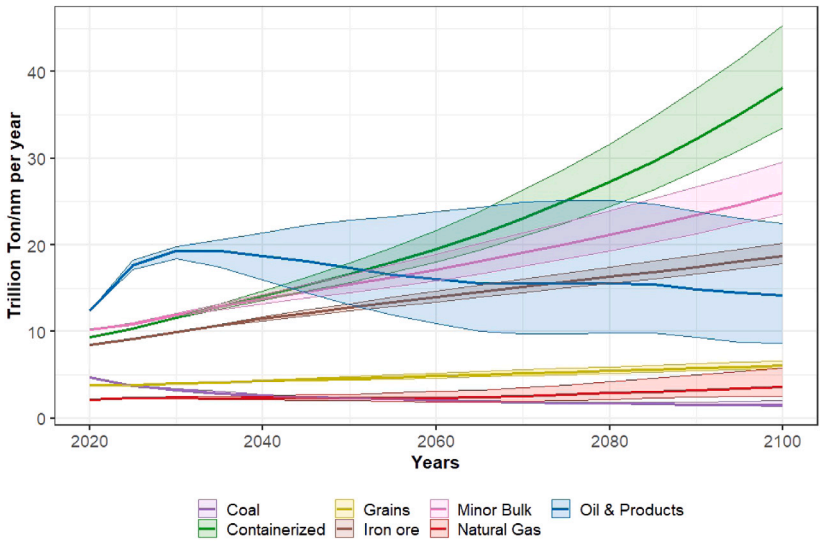

Fig. 12. The range of projected shipping demand of cargoes across scenarios.

products. This is because Europe will likely reduce its consumption of oil products, resulting in an excess oil supply in the global market and subsequently causing a reduction in global oil prices. Low-cost producers like those in the Middle East maintain or even expand production. Additionally, the increase in the export of fossil fuels from Europe to the non-taxed regions will stimulate seaborne trade. The trade of other cargoes also increases slightly due to lower global fuel prices. This will change when other regions implement carbon taxation starting in 2035 [Fig. 13]. Policymakers should aim to coordinate global efforts in implementing carbon taxes to avoid unintended regional trade imbalances and ensure fair competition. A harmonized approach to carbon taxation would prevent market distortions and unintended emission increases. As the first to implement a carbon tax in shipping, Europe should invest taxation revenues in dual-use port infrastructure and vessels adaptable to alternative energy cargoes while subsidizing cleaner shipping technologies such as carbon-neutral fuels and energy-efficient vessels. This strategy would future-proof trade routes, accelerate the global energy transition, and position Europe as a leader in decarbonizing maritime trade, balancing short-term economic gains with long-term climate goals.

- **Regardless of the scenario or the level of carbon tax imposed, shipping demand is expected to rise across multiple regions.** Sub-Saharan Africa stands out with the most substantial growth due to economic and demographic expansion. On the import side, China, Mexico, India, Canada, and LACA also show notable increases, but Sub-Saharan Africa outpaces them the all by end of the century. On the export side, Brazil and Oceania are projected to see expansion due to strong iron ore shipments and limited alternatives. LACA's diversified cargo exports and India & Mexico's focus on minor bulk cargoes further sustain overall trade growth. Because these trends persist across various scenarios, stakeholders can view these markets with higher certainty. Policymakers should prioritize investments in port infrastructure and strengthen regulatory frameworks to support these expansions. Industry leaders and investors can capitalize on the heightened certainty by adopting advanced logistics solutions and forging strategic partnerships (see Fig. 14).
- **China** maintains its upward trajectory as a major importing region across all scenarios. Its role as an exporter, particularly in minor bulk cargoes, continues to strengthen, even under mitigated scenarios. The **USA**'s position as an exporter remains resilient, though oil exports decline in mitigated scenarios. As an importer, the USA's trend — whether upward or downward — is highly dependent on the ambition level of policy measures. A similar pattern is observed in Southeast Asia, where import trends are also closely tied to policy severity.
- **Based on all scenarios, it is anticipated that coal trade will decrease over time**, while there is a likelihood of an increase in the trade of grain, iron ore, containerized cargo, and minor bulk. As for LNG and oil products, there is a high level of uncertainty, and there are more observed fluctuations in response to the global carbon tax (see Fig. 15).
- **Strengthening policy measures for decarbonization can deliver significant emissions reductions but must be balanced against potential economic impacts.** As shown in Fig. 16, stricter decarbonization measures significantly raise policy costs and drive shipping demand declines beyond what GDP losses alone would suggest. This extra drop is due in part to reduced fossil fuel trade and higher fuel prices, not just slower economic growth. The trade-off between ambitious emission targets and economic impacts is clear: stricter policies lead to deeper emissions cuts but come with significant costs to global trade and economic activity.

  Stricter taxation and the rising costs of clean technologies put pressure on the overall economy and make it harder for smaller or less financially strong companies to enter the market. As a result, larger companies that can handle these costs more easily will likely gain an advantage in challenging market conditions. Additionally, as expenses and operational challenges grow, other shipping sectors might start adopting business plans and strategies commonly used in the container shipping industry, like standardizing processes and using advanced technology, to stay competitive in this stressed market.

5. Uncertainty and future work

Scenarios and models inherently involve uncertainty due to their projective nature, as emphasized by Refsgaard et al. (2007), who differentiate between unrecognized knowledge gaps and acknowledged limitations. Walker et al. (2003) categorize this uncertainty into key areas: context and framing, input, model structure, and parameter

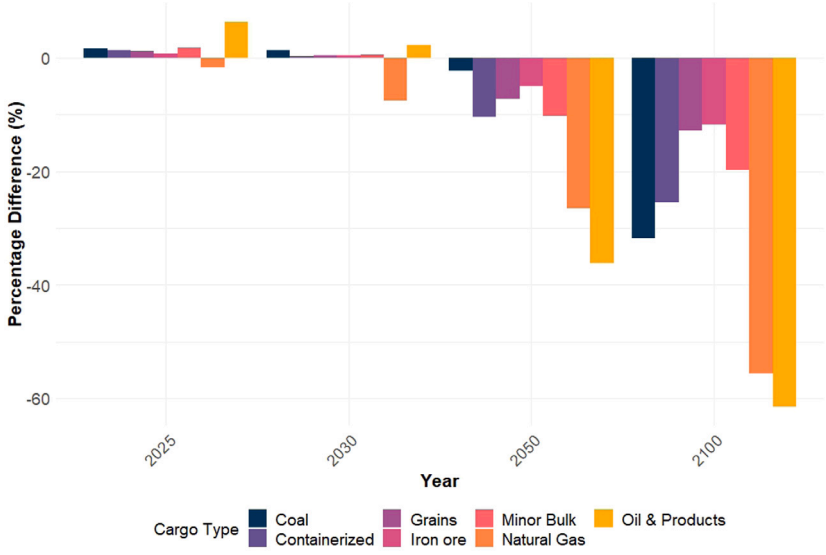

Fig. 13. Comparison of MIT-B-EU scenario with respect to baseline non-MIT scenario.

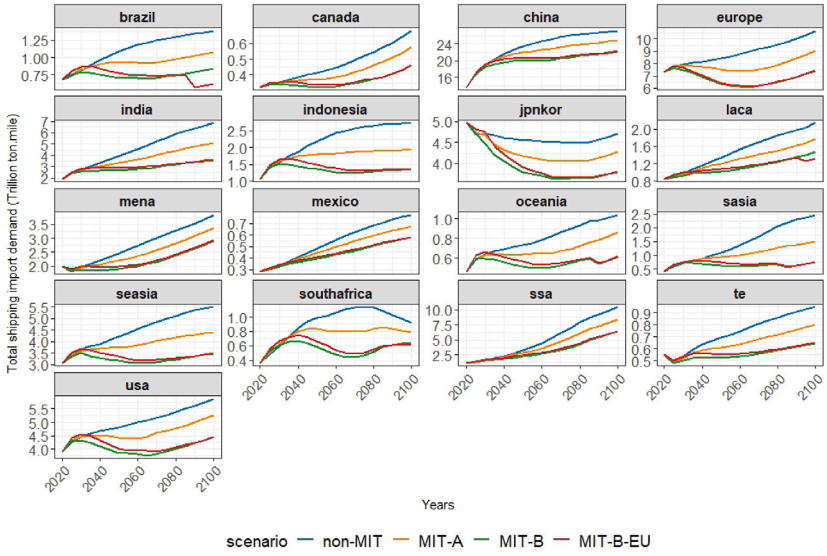

Fig. 14. Global seaborne trade in the scenarios breakdown by importing region.

uncertainties. These uncertainties complicate the assessment of scenario projections as definitively right or wrong, suggesting that some elements may be less feasible than others. Rather than focusing on absolute values, such studies should prioritize identifying trends and understanding potential impacts, offering a more actionable and strategic perspective on future developments. These models should be viewed as comparative tools rather than purely predictive ones. Despite these inherent uncertainties, this study mitigates risks by validating against existing datasets while keeping the assumption of unchanged bilateral dynamics between regions. It focuses exclusively on changes driven by climate policy without altering other relationships. The emphasis remains on understanding broader patterns, not precise predictions, which can provide valuable insights into energy transition pathways and impacts.

Several recommendations are proposed to enhance the robustness and relevance of future studies. Firstly, there should be a greater focus on exploring new trade corridors, particularly those that may emerge for renewable fuels and other cargo types that are not currently prominent, such as hydrogen and biomass. This forward-looking approach will help identify and analyze emerging trends. Secondly, applying the econometric model to multiple Integrated Assessment Models could provide a more comprehensive multi-model analysis, enabling comparisons that yield more profound insights into trade dynamics. Lastly, it is interesting to investigate the non-economical parameters such as political instability, ports' regulations, and geopolitical tensions to understand how these factors influence trade. This exploration will provide a more accurate understanding of trade patterns, but it is out of this research's scope.

Following this study, the next phase involves converting shipping demand into energy requirements. We aim to create a fuel supply model that assesses the energy needs and fuel mix of the maritime industry, offering a more transparent view of shipping's contribution to the energy transition from integrated perspectives.

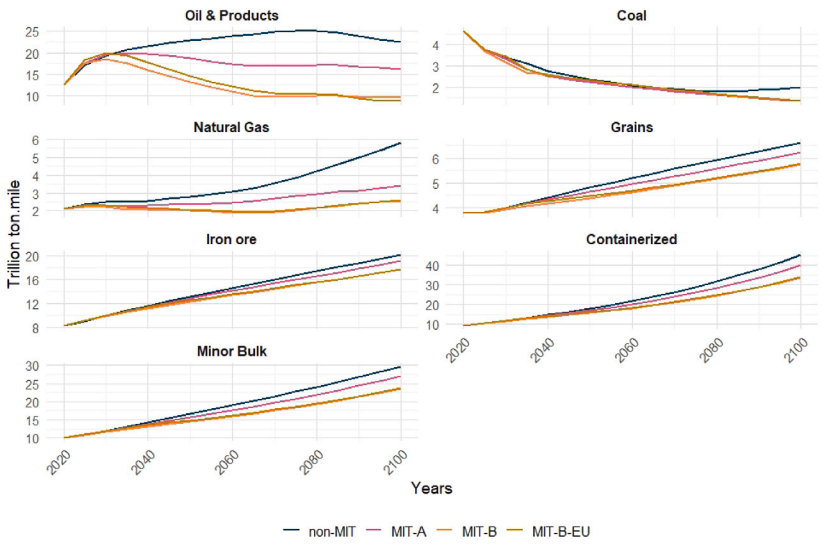

Fig. 15. Global seaborne trade in the scenarios breakdown by group of products.

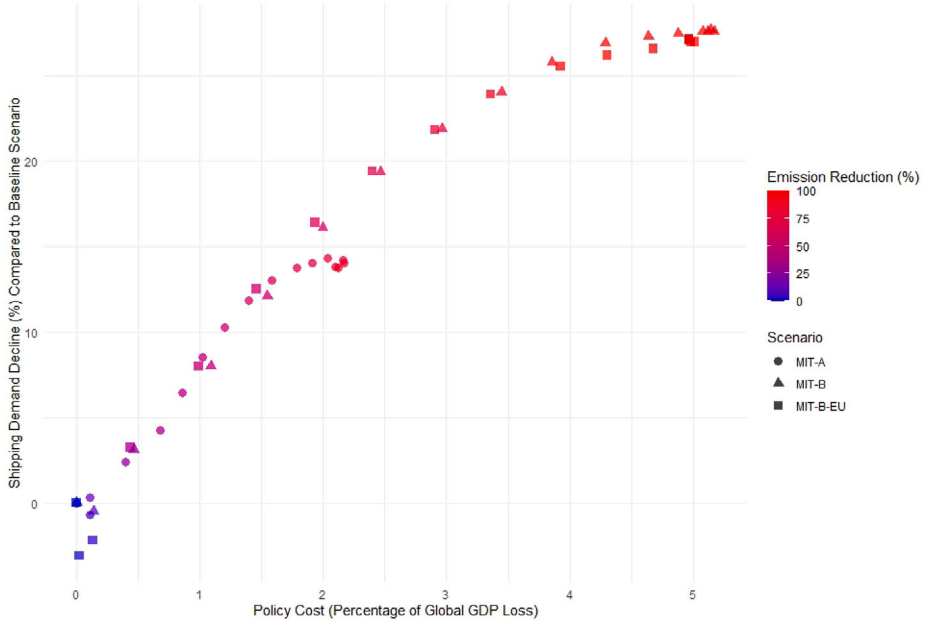

Fig. 16. Global policy costs, emission reduction, and shipping demand decline relationship.

CRediT authorship contribution statement

Hesam Naghash: Writing – review & editing, Writing – original draft, Visualization, Software, Methodology, Formal analysis, Conceptualization. **Dingena Schott:** Writing – review & editing, Supervision. **Jeroen Pruyn:** Writing – review & editing, Validation, Supervision.

Declaration of competing interest

The authors declare the following financial interests/personal relationships which may be considered as potential competing interests: Hesam Naghash reports administrative support was provided by Euro-Mediterranean Center on Climate Change. If there are other authors, they declare that they have no known competing financial interests or personal relationships that could have appeared to influence the work reported in this paper.

Acknowledgments

The research presented in this paper is part of the EU-funded Horizon 2020 project MAGPIE (sMArt Green Ports as Integrated Efficient multimodal hubs, contract No.: 101036594). We want to acknowledge all partners for their contributions. Also, we acknowledge the CMCC Foundation - Euro-Mediterranean Center on Climate Change, Italy, and RFF-CMCC European Institute on Economics and the Environment, Italy, for providing access to its supercomputer facility.

Appendix

A.1. Econometric model details

See Tables A.4–A.7.

Table A.4
Table of model specifics.

Category	Econometric model	Determinant variables	Estimation method	Data source and span
Energy	Augmented & disaggregated gravity model	GDP, Consumption, Production, Distance, Fuel price	RIDGE	bpstats 2014–2021
Non-energy Major bulk	Disaggregated gravity model	GDP, Distance, Fuel price	OLS	Trademap 2015–2021
Minor bulk and containerized	Gravity application based model & allocation distribution	GDP, Fuel price	OLS	Clarksons 2002–2021

Table A.5
Variance Inflation Factors (VIF) for different variables across energy models.

Variable	Coal (VIF)	Gas (VIF)	Crude oil (VIF)	Petroleum product (VIF)
Production_x	60.79	48.83	4.28	2.48
Consumption_i	48.77	57.83	25.68	22.73
Production_i	47.61	34.05	2.04	2.21
Consumption_x	54.15	73.10	19.72	26.14
fprice	8.54	7.26	9.11	9.56
Distance	4.78	5.49	4.91	5.09
GDP_i	3.33	8.80	15.51	14.07
GDP_x	2.47	8.20	11.10	14.99

Table A.6
Number of observations used for each cargo model.

Cargo type	Grains	Iron ore	Coal	LNG	Oil & Products	Containerized	Minor bulk
Observations	1292	1408	216	284	720	680	20

Table A.7
Variance Inflation Factors (VIF) for iron ore and grain models.

Variable	Iron ore (VIF)	Grain (VIF)
GDPX	1.84	1.74
GDPI	1.67	1.68
DISTANCE	5.84	5.62
FPRICE	5.74	5.31

Table A.8
Passability of chokepoints and canals by ship type and size. references: EIA (2017, 2024), Alexander (1992) and IEA (2024).

Chokepoint/Canal	Container ships (TEU)	Bulk carriers (DWT)	Oil tankers (DWT)
Strait of Hormuz	No restrictions; all sizes (up to 24,000+ TEU)	No restrictions; all sizes (up to 400,000 DWT)	No restrictions; ULCCs (up to 500,000 DWT) can pass
Strait of Malacca	Limited to vessels with draft ≤23 m; 20,000 TEU max	Capesize restricted; limited to 150,000 DWT	Limited to Suezmax (200,000 DWT); VLCCs with lightering
Suez Canal	Allows New Panamax (15,000 TEU) and most ULCVs	Capesize allowed with constraints; VLOCs restricted (200,000 DWT max)	Limited to Suezmax(200,000 DWT)
Panama Canal	Limited to New Panamax (≤15,000 TEU)	Capesize restricted; Panamax (80,000 DWT) and smaller allowed	Limited to Aframax (120,000 DWT) and smaller
Bab-el-Mandeb Strait	No restrictions; all sizes (up to 24,000+ TEU)	No restrictions; all sizes (up to 400,000 DWT)	No restrictions; ULCCs (up to 500,000 DWT) can pass
Danish Straits	Limited to vessels with draft ≤15 m; 5000 TEU max	Panamax (80,000 DWT) and smaller allowed	Limited to Aframax (120,000 DWT) and smaller
Turkish Straits	Limited to vessels with draft ≤15 m; 5000 TEU max	Panamax (80,000 DWT) and smaller allowed	Limited to Aframax (120,000 DWT) and smaller
Cape of Good Hope	No restrictions; all sizes (up to 24,000+ TEU)	No restrictions; all sizes (up to 400,000 DWT)	No restrictions; ULCCs (up to 500,000 DWT) can pass

A.2. Spatial matrix of distance estimation

See Tables A.8 and A.9.

A.3. Validation of the models

See Figs. A.17, A.18 and Table A.10.

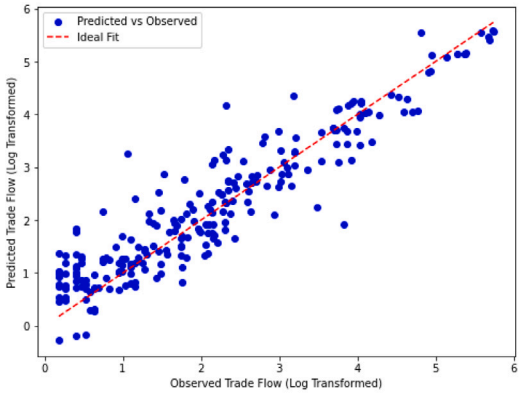

(a) Predicted trade flows vs actual observed flows for oil and petroleum products

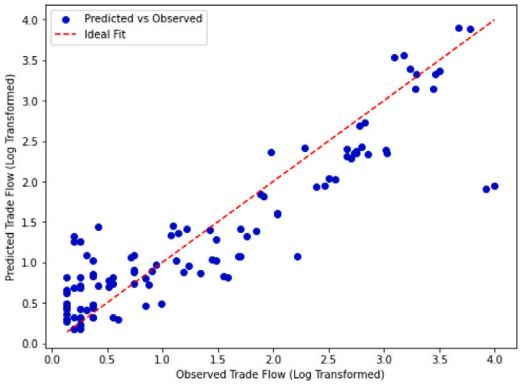

(b) Predicted trade flows vs actual observed flows for LNG

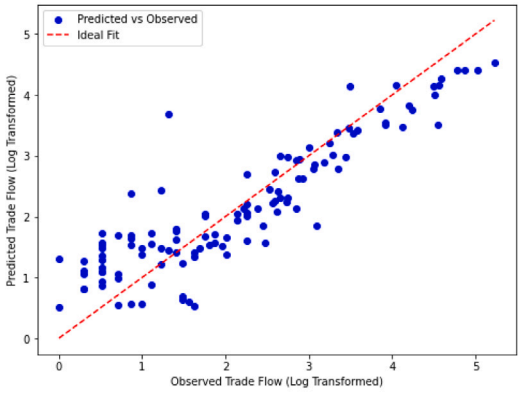

(c) Predicted trade flows vs actual observed flows for coal

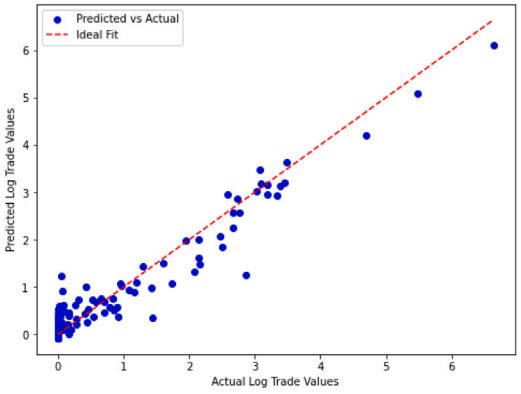

(d) Predicted trade flows vs actual observed flows for iron ore

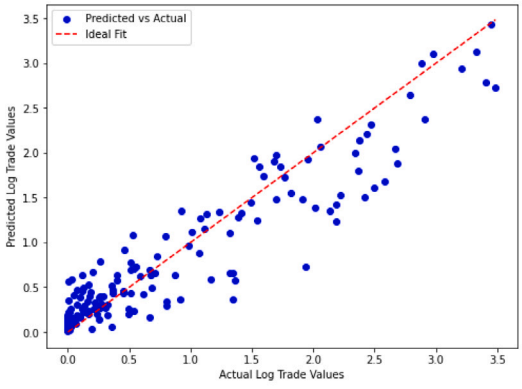

(e) Predicted trade flows vs actual observed flows for whole grains

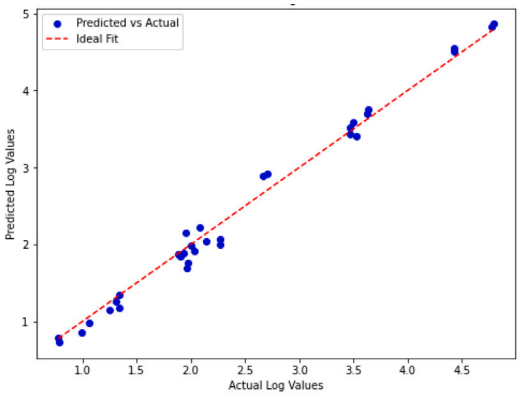

(f) Predicted trade flows vs actual observed flows for Containerized cargo

Fig. A.17. Validation results for econometric models. Each panel shows the actual versus predicted values for a specific model or cargo category. 2022 and 2023 data are used for validation.

Table A.9
Distribution of Ship Types, Capacities, and Categories. Reference: IMO (2020).

Vessel type	Vessel capacity	Size category	Distribution of ships (Capacity)
Containership [TEU]	<3k	Feeder	19%
	3–6k	Intermediate	23%
	6–8k	Intermediate	9%
	8–12k	Neo-Panamax	27%
	12–15k	Neo-Panamax	14%
	>15k	Post-Panamax	9%
Bulker [DWT]	<40k	Handysize	12%
	40-60k	Handymax	24%
	60-80k	Panamax	25%
	>80k	Capesize	39%
Tanker [DWT]	<55k	Handysize	22%
	55–85k	Panamax	6%
	85–125k	Aframax	19%
	125–200k	Suezmax	15%
	>200k	UL/VLCC	39%

Table A.10
Validation metrics for econometric models.

Model	R^2	MSE	RMSE	MAE
Oil and Petroleum products	0.859	0.289	0.538	0.401
Coal	0.792	0.359	0.599	0.475
LNG	0.818	0.240	0.490	0.356
Containerized cargo	0.987	0.017	0.132	0.109
Iron Ore	0.939	0.081	0.284	0.203
Grains	0.878	0.109	0.331	0.234

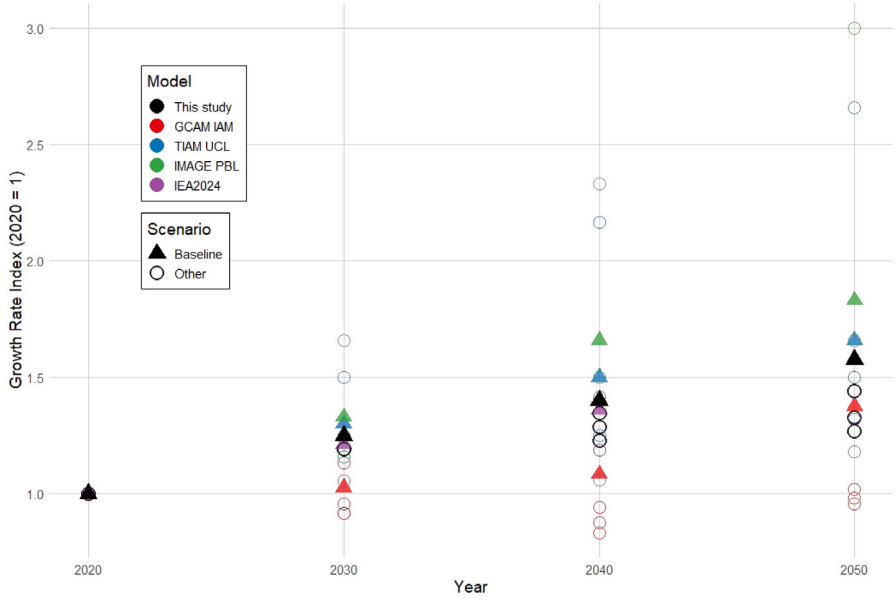

Fig. A.18. Comparison of results with those of similar works predicting future global shipping demand. References for data: GCAM IAM (Speizer et al., 2024b), TIAM UCL (Walsh et al., 2019), IMAGE PBL (Müller-Casseres et al., 2021), IEA2024 (IEA, 2024).

A.4. Scenario definition

Table A.11 and Fig. A.19 show more details of the scenarios used in the paper's analysis. The temperature increase is bound to end of the century (year 2100).

A.5. Regions mapping

Table A.12 shows the regions in the model, the actual countries they represent, and the proxy ports used for distance estimation. Canada, USA, SSA, and TE regions include two ports, one on the west and the other on the east.

Table A.11
Scenarios and carbon tax details.

Scenario	Carbon tax [$/tonCO2] (2030, 2050, 2100)	Baseline (Population & GDP)	Temp (°C)	Mitigation capacity
Non-MIT	Global: (0, 0, 0)	SSP2	~3.5	Low
MIT-A	Global: (9, 52, 135)	SSP2	~2	Mid
MIT-B	Global: (36, 239, 673)	SSP2	~1.5	High
MIT-B-EU	Europe: (36, 239, 673)Others: (0, 239, 673)	SSP2	~1.5	High

Table A.12
Regions, representations, and proxy ports.

Regions in the model	Representing	Proxy ports
CANADA	Canada	Montreal(E), Vancouver(W)
EUROPE	Western Europe	Rotterdam
JPNKOR	Japan, Korea	Chiba
MEXICO	Mexico	Manzanillo
OCEANIA	Australia, New Zealand	Brisbane
USA	United States of America	Galveston(E), Los Angeles(W)
BRAZIL	Brazil	Santos
INDIA	India	Mumbai
INDONESIA	Indonesia	Tanjung Priok
LACA	Latin America & Caribbean	Panama
MENA	Middle East & North Africa	Jebel Ali
SA	South Africa	Durban
SASIA	South Asia (Afghanistan, Pakistan)	Karachi
SEASIA	South East Asia	Singapore
SSA	Sub-Saharan Africa	Mombasa (E), Lagos (W)
TE	Eastern European Countries including Russia	Novorossiysk(W), Vostochnyy(E)

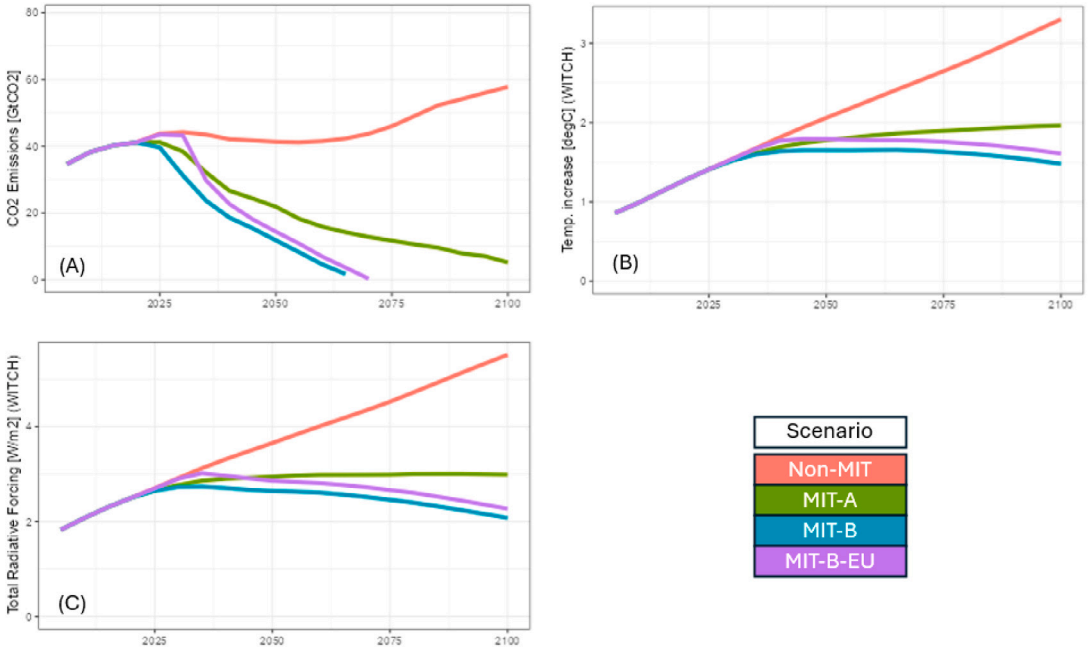

Fig. A.19. Global projections under four scenarios. (A): Global CO_2 emissions ($GtCO_2$), showing the trajectory of emissions over time. (B): Temperature increase (°C) in the atmosphere, highlighting the impact of emissions on global temperature rise. (C): Total radiative forcing (W/m^2), representing the net effect of all climate forcing components. All panels compare the outcomes of the four scenarios included in the study.

Data availability

The datasets used and/or analyzed during the current study are available from the corresponding author upon reasonable request.

References

Achakulwisut, P., Erickson, P., Guivarch, C., Schaeffer, R., Brutschin, E., Pye, S., 2023. Global fossil fuel reduction pathways under different climate mitigation strategies and ambitions. Nat. Commun. 14 (1), 5425.

Adland, R., Jia, H., Strandenes, S.P., 2017. Are AIS-based trade volume estimates reliable? The case of crude oil exports. Marit. Policy Manag. 44 (5), 657–665.

Agreement, P., 2015. UNFCCC adoption of the Paris agreement. COP. In: 25th Session Paris. Vol. 30, pp. 1–25.

Alexander, L.M., 1992. The role of choke points in the ocean context. GeoJ. 26, 503–509.

Alston, J.M., Carter, C.A., Green, R., Pick, D., 1990. Whither Armington trade models? Am. J. Agric. Econ. 72 (2), 455–467.

Babri, S., Jørnsten, K., Viertel, M., 2017. Application of gravity models with a fixed component in the international trade flows of coal, iron ore and crude oil. Marit. Econ. Logist. 19, 334–351.

BP, 2021. BP statistical review of world energy 2014–2021. URL https://www.bp.com/statisticalreview. (Accessed 30 July 2024).

Buongiorno, J., 2016. Gravity models of forest products trade: Applications to forecasting and policy analysis. Forestry 89 (2), 117–126.

Byers, E., Krey, V., Kriegler, E., Riahi, K., Schaeffer, R., Kikstra, J., Lamboll, R., Nicholls, Z., Sandstad, M., Smith, C., et al., 2022. AR6 scenarios database.

Calvin, K., Patel, P., Clarke, L., Asrar, G., Bond-Lamberty, B., Cui, R.Y., Di Vittorio, A., Dorheim, K., Edmonds, J., Hartin, C., Hejazi, M., Horowitz, R., Iyer, G., Kyle, P., Kim, S.H., Link, R., McJeon, H., Smith, S.J., Snyder, A., Waldhoff, S., Wise, M., 2019. GCAM v5.1: representing the linkages between energy, water, land, climate, and economic systems. Geosci. Model. Dev. 12, 677–698.

Chou, C.-C., Chu, C.-W., Liang, G.-S., 2008. A modified regression model for forecasting the volumes of Taiwan's import containers. Math. Comput. Modelling 47 (9–10), 797–807.

Circlaeys, S., Kanitkar, C., Kumazawa, D., 2017. Bilateral trade flow prediction. Unpublished manuscript, Available for download at http://cs229.stanford.edu/proj2017/final-reports/5240224.pdf.

Clarkson Research Services, 2024. Global shipping data. URL https://www.clarksons.net/sin/global-shipping/, Data retrieved from Clarkson Research Services. (Accessed 30 July 2024).

Comer, B., Carvalho, F., 2023. Imo's newly revised GHG strategy: what it means for shipping and the Paris agreement. Int. Counc. Clean Transp..

De Benedictis, L., Taglioni, D., 2011. The gravity model in international trade. Springer.

De Cian, E., Bosetti, V., Sgobbi, A., Tavoni, M., 2009. The 2008 WITCH model: new model features and baseline.

DNV, 2021. Maritime Forecast to 2050. Report, DNV.

DNV, G., 2022. EEXI—Energy efficiency existing ship index.

Do, Q.-T., Levchenko, A.A., Raddatz, C., 2016. Comparative advantage, international trade, and fertility. J. Dev. Econ. 119, 48–66.

EIA, U., 2017. World oil transit chokepoints. US Energy Inf. Adm..

EIA, U., 2024. World oil transit chokepoints. US Energy Inf. Adm..

Food and Agriculture Organization of the United Nations, 2024. Land, inputs and sustainability: Land use. URL https://www.fao.org/faostat/en/data/RL.

Fricko, O., Havlik, P., Rogelj, J., Klimont, Z., Gusti, M., Johnson, N., Kolp, P., Strubegger, M., Valin, H., Amann, M., et al., 2017. The marker quantification of the shared socioeconomic pathway 2: A middle-of-the-road scenario for the 21st century. Glob. Environ. Chang. 42, 251–267.

Gómez-Herrera, E., 2013. Comparing alternative methods to estimate gravity models of bilateral trade. Empir. Econ. 44, 1087–1111.

Hackmann, B., 2012. Analysis of the governance architecture to regulate GHG emissions from international shipping. Int. Environ. Agreem.: Politics Law Econ. 12, 85–103.

Han, T.-C., Wang, C.-M., 2021. Shipping bunker cost risk assessment and management during the coronavirus oil shock. Sustain. 13 (9), 4998.

Huang, Y., Rashidi, T.H., Gardner, L., 2018. Modelling the global maritime container network. Marit. Econ. Logist. 20, 400–420.

IEA, 2024. Energy Technology Perspectives 2024. IEA, Paris, URL https://www.iea.org/reports/energy-technology-perspectives-2024.

IMO, 2020. Fourth IMO ghg study 2020.

Integrated Assessment Modeling Consortium (IAMC), 2024. WITCH model resources. URL https://www.iamconsortium.org/resources/model-resources/witch/. c.

International Energy Agency, 2023. Coal 2023. URL https://www.iea.org/reports/coal-2023.

International Energy Agency, 2024. International shipping. https://www.iea.org/energy-system/transport/international-shipping. (Accessed 23 July 2024).

International Maritime Organization, 2024. EEXI and CII - ship carbon intensity and rating system. https://www.imo.org/en/MediaCentre/HotTopics/Pages/EEXI-CII-FAQ.aspx. (Accessed 26 July 2024).

Kidwell, J.S., Brown, L.H., 1982. Ridge regression as a technique for analyzing models with multicollinearity. J. Marriage Fam. 287–299.

Kottou, E.M., Grubelich, T.A., Wang, X., 2020. Bilateral trade flow prediction models enhanced by wavelet and machine learning algorithms. In: 2020 International Conference on Computational Science and Computational Intelligence. CSCI, IEEE, pp. 1510–1516.

Leamer, E.E., et al., 1995. The Heckscher-Ohlin model in theory and practice.

Li, Y., Bai, X., Wang, Q., Ma, Z., 2022. A big data approach to cargo type prediction and its implications for oil trade estimation. Transp. Res. E 165, 102831.

Mastrandrea, M.D., Mach, K.J., Plattner, G.-K., Edenhofer, O., Stocker, T.F., Field, C.B., Ebi, K.L., Matschoss, P.R., 2011. The IPCC AR5 guidance note on consistent treatment of uncertainties: a common approach across the working groups. Clim. Change 108, 675–691.

Maxwell, D., Zhu, Z., 2011. Natural gas prices, LNG transport costs, and the dynamics of lng imports. Energy Econ. 33 (2), 217–226.

Meersman, H., Van de Voorde, E., 2013. The relationship between economic activity and freight transport. In: Freight Transport Modelling. Emerald Group Publishing Limited, pp. 15–43.

Merk, O., Hoffmann, J., Haralambides, H., 2022. Post-COVID-19 scenarios for the governance of maritime transport and ports. Marit. Econ. Logist. 24 (4), 673–685.

Michail, N.A., 2020. World economic growth and seaborne trade volume: quantifying the relationship. Transp. Res. Interdiscip. Perspect. 4, 100108.

Michail, N., Melas, K.D., Batzilis, D., 2021. Container shipping trade and real GDP growth: A panel vector autoregressive approach. Econ. Bull. 41 (2), Nektarios A. Michail Konstantinos D. Melas Dimitris Batzilis, (2021) Container shipping trade and real GDP growth: A panel vector autoregressive approach.

Minakawa, N., Izumi, K., Sakaji, H., 2022. Bilateral trade flow prediction by gravity-informed graph auto-encoder. In: 2022 IEEE International Conference on Big Data (Big Data). IEEE, pp. 2327–2332.

Müller-Casseres, E., Edelenbosch, O.Y., Szklo, A., Schaeffer, R., van Vuuren, D.P., 2021. Global futures of trade impacting the challenge to decarbonize the international shipping sector. Energy 237, 121547.

Müller-Casseres, E., Leblanc, F., van den Berg, M., Fragkos, P., Dessens, O., Naghash, H., Draeger, R., Le Gallic, T., Tagomori, I.S., Tsiropoulos, I., et al., 2023. International shipping in a world below 2C. Nat. Clim. Chang..

Naghash, H., Schott, D., Pruyn, J., 2024. Shifting waves of shipping: a review on global shipping projections and methodologies. J. Shipp. Trade 9 (1), 1–43.

O'Neill, B.C., Kriegler, E., Ebi, K.L., Kemp-Benedict, E., Riahi, K., Rothman, D.S., Van Ruijven, B.J., Van Vuuren, D.P., Birkmann, J., Kok, K., et al., 2017. The roads ahead: Narratives for shared socioeconomic pathways describing world futures in the 21st century. Glob. Environ. Chang. 42, 169–180.

Pye, S., Butnar, I., Cronin, J., Welsby, D., Price, J., Dessens, O., Rodríguez, B.S., Winning, M., Anandarajah, G., Scamman, D., Keppo, I., 2020. The TIAM-UCL Model (Version 4.1.1) Documentation. Technical Report Version 4.1.1, UCL Energy Institute.

Raucci, C., McKinlay, C., Karan, A., 2023. The Future of Maritime Fuels: What You Need to Know.

Refsgaard, J.C., van der Sluijs, J.P., Højberg, A.L., Vanrolleghem, P.A., 2007. Uncertainty in the environmental modelling process–a framework and guidance. Environ. Model. Softw. 22 (11), 1543–1556.

Riahi, K., Bertram, C., Huppmann, D., Rogelj, J., Bosetti, V., Cabardos, A.-M., Deppermann, A., Drouet, L., Frank, S., Fricko, O., et al., 2021. Cost and attainability of meeting stringent climate targets without overshoot. Nat. Clim. Chang. 11 (12), 1063–1069.

Riahi, K., Van Vuuren, D.P., Kriegler, E., Edmonds, J., O'neill, B.C., Fujimori, S., Bauer, N., Calvin, K., Dellink, R., Fricko, O., et al., 2017. The shared socioeconomic pathways and their energy, land use, and greenhouse gas emissions implications: An overview. Glob. Environ. Chang. 42, 153–168.

Samir, K., Lutz, W., 2017. The human core of the shared socioeconomic pathways: Population scenarios by age, sex and level of education for all countries to 2100. Glob. Environ. Chang. 42, 181–192.

Sea Distances, 2024. Online distance calculator. URL https://sea-distances.org/. (Accessed 30 July 2024).

Serra, P., Fadda, P., Fancello, G., 2020. Investigating the potential mitigating role of network design measures for reducing the environmental impact of maritime chains: The mediterranean case. Case Stud. Transp. Policy 8 (2), 263–280.

Siliverstovs, B., Schumacher, D., 2009. Estimating gravity equations: to log or not to log? Empir. Econ. 36, 645–669.

Silva, J.S., Tenreyro, S., 2006. The log of gravity. Rev. Econ. Stat. 88 (4), 641–658.

Speizer, S., Fuhrman, J., Aldrete Lopez, L., George, M., Kyle, P., Monteith, S., McJeon, H., 2024a. Integrated assessment modeling of a zero-emissions global transportation sector. Nat. Commun. 15 (1), 4439.

Speizer, S., Fuhrman, J., Aldrete Lopez, L., et al., 2024b. Integrated assessment modeling of a zero-emissions global transportation sector. Nat. Commun. 15, 4439. http://dx.doi.org/10.1038/s41467-024-48424-9.

Sun, J., Suo, Y., Park, S., Xu, T., Liu, Y., Wang, W., 2018. Analysis of bilateral trade flow and machine learning algorithms for GDP forecasting. Eng. Technol. Appl. Sci. Res. 8 (5).

Tang, S., Xu, S., Gao, J., 2019. An optimal model based on multifactors for container throughput forecasting. KSCE J. Civ. Eng. 23 (9), 4124–4131.

Thompson, C.G., Kim, R.S., Aloe, A.M., Becker, B.J., 2017. Extracting the variance inflation factor and other multicollinearity diagnostics from typical regression results. Basic Appl. Soc. Psychol. 39 (2), 81–90.

Tokuşlu, A., 2020. Analyzing the energy efficiency design index (EEDI) performance of a container ship. Int. J. Environ. Geoinform. 7 (2), 114–119.

Trade Map, 2024. Trade map - international trade statistics. https://www.trademap.org/Index.aspx.

Ubøe, J., Andersson, J., Jörnsten, K., Strandenes, S.P., 2009. Modeling freight markets for coal. Marit. Econ. Logist. 11, 289–301.

UNCTAD, 2021. Review of Maritime Transport. United Nations Publications, New York.

UNCTAD, 2022. Review of maritime transport. United Nations Publications, New York.

Van Beek, L., Hajer, M., Pelzer, P., van Vuuren, D., Cassen, C., 2020. Anticipating futures through models: the rise of integrated assessment modelling in the climate science-policy interface since 1970. Glob. Environ. Chang. 65, 102191.

Van Vuuren, D.P., Kok, M., Lucas, P.L., Prins, A.G., Alkemade, R., van den Berg, M., Bouwman, L., van der Esch, S., Jeuken, M., Kram, T., et al., 2015. Pathways to achieve a set of ambitious global sustainability objectives by 2050: explorations using the IMAGE integrated assessment model. Technol. Forecast. Soc. Change 98, 303–323.

Walker, W.E., Harremoës, P., Rotmans, J., Van Der Sluijs, J.P., Van Asselt, M.B., Janssen, P., Krayer von Krauss, M.P., 2003. Defining uncertainty: a conceptual basis for uncertainty management in model-based decision support. Integr. Assess. 4 (1), 5–17.

Walsh, C., Lazarou, N.-J., Traut, M., Price, J., Raucci, C., Sharmina, M., Agnolucci, P., Mander, S., Gilbert, P., Anderson, K., 2019. Trade and trade-offs: Shipping in changing climates. Mar. Policy 106, 103537.

Weyant, J., 2017. Some contributions of integrated assessment models of global climate change. Rev. Environ. Econ. Policy.

WITCH Model Development Team, 2024. WITCH model documentation. URL https://doc.witchmodel.org/. (Accessed 30 July 2024).

Wohl, I., Kennedy, J., 2018. Neural Network Analysis of International Trade. US International Trade Commission, Washington, DC, USA.

World Bank, 2024. GDP (current US). URL https://data.worldbank.org/indicator/NY.GDP.MKTP.CD. (Accessed 30 July 2024).

Zhang, H.-Y., Ji, Q., Fan, Y., 2015. What drives the formation of global oil trade patterns? Energy Econ. 49, 639–648.

Zhang, H.-Y., Xi, W.-W., Ji, Q., Zhang, Q., 2018. Exploring the driving factors of global LNG trade flows using gravity modelling. J. Clean. Prod. 172, 508–515.